SYNTHESIS AND CHARACTERIZATION OF POLYETHYLENE GLYCOL COATED MAGNETIC NANOPARTICLES AND THEIR USE FOR ANTI-CANCER DRUG DELIVERY

A THESIS SUBMITTED TO
THE GRADUATE SCHOOL OF NATURAL AND APPLIED SCIENCES
OF
MIDDLE EAST TECHNICAL UNIVERSITY

BY

MURAT ERDEM

IN PARTIAL FULFILLMENT OF THE REQUIREMENTS
FOR
THE DEGREE OF MASTER OF SCIENCE
IN
BIOLOGY

AUGUST 2014

Approval of the thesis

SYNTHESIS AND CHARACTERIZATION OF POLYETHYLENE GLYCOL COATED MAGNETIC NANOPARTICLES AND THEIR USE FOR ANTI-CANCER DRUG DELIVERY

submitted by **MURAT ERDEM** in partial fulfillment of the requirements for the degree of **Master of Science in Biology Department, Middle East Technical University** by,

Prof. Dr. Canan Özgen _____
Dean, Graduate School of **Natural and Applied Sciences**

Prof. Dr. Orhan Adalı _____
Head of Department, **Biology**

Prof. Dr. Ufuk Gündüz _____
Supervisor, **Biology Dept., METU**

Assist. Prof. Dr. Serap Yalçın Azarkan _____
Co-supervisor, **Food Eng. Dept., AHİ EVRAN UNİ.**

Examining Committee Members:

Assoc. Prof. Dr. Dilek (Şendil) Keskin _____
Engineering Sciences Dept., METU

Prof. Dr. Ufuk Gündüz _____
Biology Dept., METU

Assoc. Prof. Dr. Mayda Gürsel _____
Biology Dept., METU

Assoc. Prof. Dr.Çağdaş Devrim Son _____
Biology Dept., METU

Dr. Pelin Mutlu _____
METU Central Lab, Molecular Bio. and Biotech. R&D

Date: 28.08.2014

I hereby declare that all information in this document has been obtained and presented in accordance with academic rules and ethical conduct. I also declare that, as required by these rules and conduct, I have fully cited and referenced all material and results that are not original to this work.

Name, Last name: MURAT ERDEM

Signature:

ABSTRACT

SYNTHESIS AND CHARACTERIZATION OF POLYETHYLENE GLYCOL COATED MAGNETIC NANOPARTICLES AND THEIR USE FOR ANTI-CANCER DRUG DELIVERY

Erdem, Murat

M.S., Department of Biology

Supervisor: Prof. Dr. Ufuk Gündüz

Co-supervisor: Assist. Prof. Dr. Serap Yalçın Azarkan

August 2014, 73 pages

Although conventional chemotherapy is the most valid method to cope with cancer, it has many drawbacks such as decrease in production of blood cells, inflammation of the lining of the digestive tract, hair loss etc. Reasons for its side effects are that drugs used in chemotherapy are distributed evenly within the body of a patient and cannot distinguish the cancer cells from the healthy ones. To decrease the negative effects of chemotherapeutic drugs and to increase their efficiency, many drug delivery systems have been developed until now. Magnetic nanoparticles have an important potential for cancer treatment. The most significant feature of magnetic nanoparticles is that they can be manipulated for targeting to tumor side by application of external magnetic field. Also, their small size and their capability to carry drug by surface modification are other important characteristics for drug delivery.

Aim of this study is to synthesize folic acid conjugated, polyethylene coated magnetic nanoparticles (FA-MNPs) and doxorubicin loaded formulation (Dox-FA-MNPs), and to

investigate their cytotoxicity on HeLa and doxorubicin resistant HeLa cells. Magnetic nanoparticles (MNPs), PEG coated MNPs and FA-MNPs were successfully synthesized and characterized by one or more of TEM, FTIR, XRD, TGA and VSM analysis. Doxorubicin (Dox) loading capacity of FA-MNPs and release profile of Dox from Dox-FA-MNPs were investigated by spectrometer. Internalization of FA-MNPs and Dox-FA-MNPs by HeLa cells were observed by purssian blue staining under light microscopy and by using fluorescent property of Dox under fluorescent microscopy respectively. Biocompatibility of FA-MNPs and antiproliferative effects of Dox-FA-MNPs on HeLa and HeLa/Dox cells were analyzed by XTT cell proliferation assay.

The results show that synthesis of MNPs, PEG-MNPs and FA-MNPs were successfully achieved. MNPs had a special shape and small size and also had supermagnetic behavior. 505 μM of 1724 μM Dox was loaded 500 μg/mL FA-MNPs and in 24 h, 68,35 μM Dox was released from 500 μg/mL Dox-FA-MNPs. Also, drug release was increased in acidic condition from Dox-FA-MNPs. Internalization experiments showed that FA-MNPs and Dox-FA-MNPs were taken up by HeLa cells. FA-MNPs and Dox-FA-MNPs were given to HeLa and HeLa/Dox cells for investigation of their cytotoxicities. Cell proliferation assay results showed that Dox-FA-MNPs significantly decreased the proliferation of HeLa cells when compared to FA-MNPs. However, Dox-FA-MNPs did not show same effects on HeLa/Dox cells.

Despite that Dox-FA-MNPs could not overcome drug resistance of HeLa/Dox cells, they effectively killed HeLa cells. As a result, FA-MNPs have found to be important for carrying Dox.

Keywords: Cancer, HeLa, drug delivery system, magnetic nanoparticles

ÖZ

POLİETİLEN GLİKOL KAPLI MANYETİK NANOPARÇACIKLARIN SENTEZİ VE KARAKTERİZASYONU VE ANTİ-KANSER İLAÇ TAŞINMASINDA KULLANIMI

Erdem, Murat

Yüksek Lisans, Biyoloji Bölümü

Tez Yöneticisi: Prof. Dr. Ufuk Gündüz

Ortak Tez Yöneticisi: Assist. Prof. Dr. Serap Yalçın Azarkan

Ağustos 2014, 73 sayfa

Geleneksel kemoterapi kanserle baş etmede en geçerli metot olmasına rağmen kemoterapinin kan hücresi üretiminde azalma, sindirim sistemi zarının inflamasyonu, saç dökülmesi gibi bir çok yan etkisi bulunmaktadır. Bu yan etkilerin nedeni kemoterapide kullanılan ilaçların hastanın bedeninde eşit şeklide dağılması ve ilacın kanser hücrelerini sağlıklı hücrelerden ayırt etmemesidir. Kemoterapötik ilaçların olumsuz etkilerini azaltmak ve verimliliği artırmak için, şimdiye kadar birçok ilaç taşıma sistemi geliştirilmiştir. Manyetik nanoparçacıklar kanser tedavisi için önemli bir potansiyele sahiptir. Manyetik nanoparçacıkların en önemli özelliği, harici bir manyetik alanın uygulanmasıyla tümör bölgesine hedeflenebilmesidir. Ayrıca, manyetik nanoparçacıkların küçük boyutlu olmaları ve yüzey modifikasyonu ile ilaç taşıma kapasitesi kazanabilmeleri, ilaç taşımacalığı için gerekli diğer önemli özellikleridir.

Bu çalışmanın amacı, folik asit bağlı, polietilen glikol kaplı manyetik nanoparçacıklar (FA-MNP'ler) ve onların doksorubisin yüklü formülasyonunu (Dox-FA-MNP'ler)

sentezlemek ve bu parçacıkların doksorubisine duyarlı HeLa ve doksorubisine dirençli HeLa (HeLa/Dox) hücrelerindeki sitotoksisitelerini araştırmaktır. Manyetik nanoparçacıklar (MNP'ler), PEG kaplanmış MNP'ler (PEG-MNP'ler) ve FA-MNP'ler başarılı bir şekilde sentezlenmiş ve TEM, FTIR, XRD, TGA ve VSM analizlerinden biri ya da daha fazlası ile karakterize edilmiştir. FA-MNP'lerin doksorubisin (Dox) yükleme kapasitesi ve Dox-FA-MNP'lerin Dox salma profili spektrometre ile incelenmiştir. FA-MNP ve Dox-FA-MNP'lerin HeLa hücreleri tarafından hücre içine alımı sırasıyla ışık mikroskobu altında purssian mavi boyama yöntemiyle ve Dox'un floresan özelliği kullanılarak floresan mikroskobu altında gözlenmiştir. HeLa ve HeLa/Dox hücrelerine FA-MNP'lerin biyouyumluluğu ve Dox-FA-MNP'lerin bu hücrelerin çoğalmasına karşı etkileri, XTT-hücre proliferasyon deneyi ile analiz edilmiştir.

Sonuçlar MNP'lerin, PEG-MNP'lerin ve FA-MNP'lerin sentezinin başarılı bir şekilde gerçekleştirldiğini göstermektedir. İncelemeler, MNP'lerin özel bir şekle sahip olduğunu, küçük boyutlu olduğunu ve süperparamanyetik davranış sergilediği göstermiştir. 500 µg/mL FA-MNP'ye 505 µM Dox'un yüklendiği ve 24 saat içinde, 68,35 µM Dox'un Dox-FA-MNP'lerden salımdığı görülmüştür. Aynı zamanda, ortamın asitliliği 500µg/mL Dox-FA-MNP'lerin ilaç salımını arttırmıştır. Mikrosopi ile yapılan gözlemler, FA-MNP'lerin ve Dox-FA-MNP'lerin HeLa hücreleri tarafından alındığını göstermiştir. FA-MNP'lerin ve Dox-FA-MNP'lerin sitotoksisite analizleri HeLa ve HeLa/Dox hücreleri ile yapılmıştır. Hücre çoğalma analizi sonuçları FA-MNPS ile karşılaştırıldığında–Dox-FA-MNP'lerin HeLa hücrelerinin çoğalmasını önemli ölçüde azalttığını göstermiştir. Ancak, Dox-FA-MNP'ler HeLa/Dox hücreleri üzerinde aynı etkiyi gösterememiştir.

Dox-FA-MNP'ler HeLa/Dox hücrelerinin ilaç dirençliliğinin geri çevrilmesinde etkili olmamasına rağmen, HeLa hücrelerini etkili bir şekilde öldürmüşlerdir. Sonuç olarak, FA-MNP'lerin Dox taşıması için önemli olduğu bulunmuştur.

Anahtar Sözcükler: Kanser, HeLa, ilaç taşıma sistemi, manyetik nanoparçacık

To My Sisters: Fatma and Safiye,

ACKNOWLEDGEMENTS

I would like to express my special appreciation and thanks to my supervisor Prof. Dr. Ufuk Gündüz for her endless support, priceless advice, and immense knowledge throughout the thesis.

I would like to thank to my co-supervisor Assist. Prof. Dr. Serap Yalçın Azarkan for her support and suggestions.

I would like to express the deepest appreciation to the members of examining committee, Assoc. Prof. Dr. Dilek Şendil Keskin, Assoc. Prof Dr. Mayda Gürsel, Assoc. Prof Dr. Çağdaş Devrim Son and Dr. Pelin Mutlu.

I am deeply thankful to Çağrı Urfalı, Ayça Nabioğlu, Gözde Ünsoy, Maryam Persian and Negar Taghavi for their experience and advices. Special thanks to my everlasting lab-mate Aktan Alpsoy for his valuable friendship, encouragement and support.

I am thankful to previous members of Lab206 Neşe Çakmak, Esra Kaplan, Ahu İzgi, Tuğba Keskin, Gülistan Tansık, Zelha Nil, Okan Tezcan, Burcu Özsoy, Gülşah Pekgöz and Çiğdem Şener.

This study is supported by METU Research Fund (Grant ID: BAP-07-02-2012-101).

TABLE OF CONTENTS

LIST OF TABLES

TABLES

LIST OF FIGURES

FIGURES

LIST OF ABBREVIATIONS

ATR	Attenuated Total Reflection
DCC	Drug delivery system
DMSO	Dimethyl sufoxide
Dox	Doxorubicin
Dox-FA-MNP	Dox loaded magnetic nanoparticle
FA-MNP	Folic acid conjugated magnetic nanoparticle
$Fe(acac)_3$	Iron(III) acetylacetonate
FTIR	Fourier Transform Infrared Spectroscopy
HeLa/Dox	500 nM Doxorubicin-resistant HeLa cell line
IC_{50}	Inhibitory concentration-50
MNP	Magnetic nanoparticle
MRI	Magnetic resonance imaging
MDR	Multidrug resistance
MDR1	Multidrug resistance protein 1
OL-Fe_3O_4	Oleic acid and oleylamine coated Fe_3O_4
PBS	Phosphate-buffered saline
PEG	Poly ethylene glycol
PEG-MNP	PEG coated magnetic nanoparticle
RES	Reticuloendotelial system
TEM	Transmission electron microscopy
TGA	Thermal gravimetric analysis
Tris	Tris(hydroxymethyl)aminomethane

VSM	Vibrating sample magnetometer
XTT	2,3-Bis-(2-Methoxy-4-Nitro-5-Sulfophenyl)-2H-Tetrazolium-5-Carboxanilide

CHAPTER 1

INTRODUCTION

1.1 Cancer

Cancer is defined as a group of more than 100 diseases which has two main characteristics, uncontrolled growth of the cells and the ability of these cells to migrate from the original site and to spread to distant sites (American Cancer Society, 2013b).

There are two main groups of genes that trigger the development of cancer. Normally, these genes have roles in the regulation of cell cycle, cell growth and cell division. First group of genes is proto-oncogenes that promote the cell to divide while the other gene group is called tumor-suppressor genes which have a role in inhibition of cell proliferation. By working together both gene groups provide cells to grow and to divide in regulated manner, so the cells function normally and meet their responsibilities for the healthy body. If mutations occur in proto-oncogenes and tumor-suppressor genes, proto-oncogenes turn into oncogenes and tumor-suppressor genes lose their function. Oncogenes cause cells to proliferate irregularly while inactivated tumor-suppressor genes cannot control the cell division. Thus, mutations occurred in these gene groups are the main causes for the abnormal cell proliferation observed in cancers. Unlike normal cell acts, cancer cells grow and proliferate irregularly. Then, they colonize in healthy tissues and organs. Finally they metastasize the body (National Institutes of Health, 2007).

1.2 Cervical Cancer

According to GLOBOCAN 2013, cancer incidence among women was recorded as 6.0447 million in worldwide in 2008. Cervical cancer is accounted for 275 000 deaths worldwide in 2008. Cervical cancer is the third common cancer types globally occurring among women.

Cervical cancer occurs in the cervix which is the organ located between the uterus and vagina. It is usually a slow-growing cancer that may not have symptoms but can be found with regular Pap tests (a procedure in which cells are scraped from the cervix and looked at under a microscope). Cervical cancer is almost always caused by human papillomavirus infection (National Cancer Institute, 2013a).

1.3 Treatment Options for Cervical Cancer

Cervical cancer has some different treatment options which are the currently used treatments and tested treatments in laboratories and clinical trials. Standard treatments are surgery, radiotherapy and chemotherapy. Developing methods are research studies to improve current treatments or obtain information on new treatments for cervical cancer. If the research studies on treatment of cervical cancer show better results than the current treatments, the new treatment could be the standard treatment (National Cancer Institute, 2013b).

1.3.1 Surgery

The most common method for the treatment of many different cancer types is surgery which is the removal of affected area and surrounding tissue. Three main types of

surgery which are applied to cervical cancer are radical trachelectomy, hysterectomy and pelvic exenteration. Firstly, radical trachelectomy is the operation which includes the removal of the cervix, surrounding tissue and the upper part of the vagina but not the womb. Secondly, in hysterectomy, the cervix and womb are removed while depending on the stage of the cancer, the ovaries and fallopian tubes may also be necessary to be removed. Finally, pelvic exenteration is a major operation which removes the cervix, vagina, womb, bladder, ovaries, fallopian tubes and rectum (Health News Stories, 2013).

After surgery, patients could experience some side effects. First one is urination problem. Women may have feeling that they could not urinate. Secondly, the removal of ovary might cause women to enter menopause. Thirdly, if during surgery, lymph nodes are removed, swelling occurs in legs due to the malfunction in lymphatic systems. Also, women may experience physical and emotional changes, so their feeling about sex may be affected (Cancer Council Victoria, 2013).

1.3.2 Radiation Therapy

Radiation therapy provides cervical cancer patients high-energy rays to destroy cancer cells. Radiation therapy can be applied cervical cancer patients in any stages. Instead of surgery, radio therapy may be used on patients in early stage of cervical cancer. Also, it could be applied to kill any cancer cells left in the area after surgery. Radiation therapy with chemotherapy may be used to kill cancer that spread out side of the cervix. Radiation therapy could be applied to patients internally, externally or together. In external radiation therapy radiation is focused on patients' pelvis or other cancerous areas while in internal radiation therapy called brachy therapy, a radioactive substance

is given to patients via a narrow cylinder located inside their vagina (National Cancer Institute, 2012).

1.3.3 Chemotherapy

Chemotherapy is the treatment of cancer by anti-neoplastic drugs. These drugs also called chemotherapeutic drugs are used to destroy rapidly dividing cancer cells (Mandal, 2014). Chemotherapy could be used alone or it can be applied to patients with other cancer treatments, such as radiation therapy or surgery. Chemotherapy could reduce the size of a tumor before the application of other therapies. Also, it can kill cancer cells that are left after surgery or that escape from radiation therapy. Chemotherapy increases the influence of radiation therapy on cancer. Moreover, chemotherapy aims to prevent recurrence of cancer and metastasis of cancer (Wedro, 2014).

Chemotherapeutic drugs can be applied in many ways. They can be orally administered as a pill. They can be injected into the muscle or fat tissue or they can be intravenously given to cancer patients. Moreover, these drugs can be applied to the skin. Also, they can be injected directly into a body cavity. Chemotherapeutic drugs can be divided into several groups depending on mechanisms of their action, their chemical structure, and their relationship with another drug. These groups are alkylating agents, antimetabolites, anti-tumor antibiotics, topoisomerase inhibitors, mitotic inhibitors and corticosteroids. Alkylating agents prevent the proliferation of cancer cells by binding covalently their alkyl groups to DNA molecules. These agents work effectively in all phases of the cell cycle by damaging DNA. Sometimes they can cause acute leukemia because their long-term usage could be harmful to the bone marrow. Antimetabolites inhibit DNA and RNA synthesis by substituting nucleic acids. These agents are toxic to

cells and prevent the cell division at the S phase. Anti-tumor antibiotics also known as anthracyclines interfere with enzymes that have roles in DNA replication. They are effective in all phases of the cell cycle. Use of these agents in high doses can cause permanent damage to the heart. Topoisomerase inhibitors prevent topoisomerases from helping separation of DNA strands during replication. Treatment with these inhibitors could cause a second cancer such as acute myelogenous leukemia. Mitotic inhibitors are generally plant alkaloids acquired from natural products. These drugs can inhibit mitosis by preventing enzymes that have roles in production of proteins required for cell division. Although they are mainly effective at M phase of the cell cycle, these agents could kill cells in any phases. These drugs can damage peripheral nerve. Corticosteroids are hormones naturally produced in body and hormone-like drugs which can be helpful in killing cancer cells. They are used to treat lymphoma, leukemia, and multiple myeloma.

Chemotherapy uses more than one drug together to treat cervical cancer because combination of drugs has more effective in killing cervical cancer cells. Drugs mostly used in cervical cancer are cisplatin, carboplatin, paclitaxel, topotecan and gemcitabine. Cisplatin and carboplatin are platinum drugs but sometimes they are classified as alkylating agents because even they do not have alkyl group, they affect cancer cells as alkylating agents do. Paclitaxel belongs to the family of mitotic inhibitors. Topotecan is a topoisomerase inhibitor while gemcitabine is in the group of antimetabolites (American Cancer Society, 2013a).

1.3.4 Side effects of Chemotherapy

Chemotherapy mainly affects the rapidly growing and dividing cells. This feature defines cancerous cells, but it can be seen in healthy cells that also actively grow and

proliferate. Such cells are found in the blood, mouth, intestines, and hair. Chemotherapy causes the side effects when it causes damages to these normal cells because chemotherapy cannot distinguish the cancer cells from the healthy ones. These side effects cause patients to suffer fatigue (tiredness), pain in different parts of body, sores in the mouth and throat, diarrhea, nausea and vomiting, blood disorders due to decrease in blood cell number, nerve damage, changes in thinking and memory, sexual and reproductive issues, appetite loss and hair loss. Also, chemotherapy causes long-term side effects. After chemotherapy treatment ends, most of draw backs do not sustain while, some effects may continue, or appear back, or later. For example, particular chemotherapeutics are responsible for persistent damage to some organs such as the heart, lung, liver, kidneys, or reproductive system. Moreover, it takes months and years for cognitive functions work properly after treatment. Changes in nervous system also can occur after treatment, and patients who were treated with chemotherapy in childhood could be exposed to late effects. The possibility of occurrence of second cancer is high for patients that beat cancer before (Schuchter, 2014).

The main problem that makes chemotherapy less effective in cancer treatment is the drug resistance. Cancer cells could be intrinsically resistant to chemotherapy drugs or initially sensitive cancer cells can become drug resistant during application of chemotherapy. Acquired resistant cancer cells become not only resistant to a certain chemotherapeutic drug but also resistant to chemically different kinds of drugs. Cancer cell can become resistant to chemotherapy drug in many ways, by elevating drug efflux and reducing drug influx; drug inactivation; alterations in drug target; processing of drug-induced damage; and evasion of apoptosis (Longley & Johnston, 2005). From them, the most important reason for multidrug resistance is that P-glycoprotein as product of MDR1 gene is expressed in a high level. This transporter protein reduces intracellular drug concentration by pumping out of the drug, so it causes a reduce in the cytotoxic effect of drug (Di Pietro et al., 1999).

1.4 Targeted Therapy

Targeted therapy means that a drug is designed to kill only cancer cells; but not healthy cells, by targeting a specific protein only found in cancer cells, not in normal cells. This therapy differentiates conventional chemotherapy by their selective cytotoxicity to cancer cells (Wu, Chang, & Huang, 2006). Determination of antibody that selectively binds cancer specific antigen gains importance in targeting a chemotherapy drug to cancer cells. For instance, anti-CD33–calicheamicin is one of the antibody-drug conjugates. It is composed of anti-CD33 antibody that specifically binds CD33 a trasmembrane protein overexpressed in acute myeloid leukemia and calicheamicin which attaches DNA and causes strand scission. Anti-CD33–calicheamicin is accepted to be used to treat acute myeloid leukemia (Chari, 2008).

1.5 Drug Delivery Systems

Drug delivery system (DDS) is a platform that introduces a chemotherapy agent to body and enhance the influence and safety of the drug in a way in which it can determine how long, how fast and where drug release occurs in the body (Attama, Momoh, & Builders, 2012). Conventional chemotherapeutic drugs are spread out evenly within the body; as a result, they have effect not only on cancer cells but also on healthy cells. Due to this even distribution of these drugs, cancerous tissue gets limiting dose of the drugs. Increase in the dose of the drug to kill more cancer cells causes the excessive toxicity to body (Cho, Wang, Nie, Chen, & Shin, 2008). To solve these problems, DDSs have been designed to increase influence of chemotherapy drug and decrease their toxicity by not only providing increment of drug accumulation in tumor site but also lowering quantity of drug distributed to healthy parts of body (Needham & Dewhirst, 2001).

The most important feature of DDSs is that drugs in the systems are released in a controlled manner. Until now, many new DDSs have been developed such as capsules, polymers, liposomes, microparticles and nanoparticles. These systems must carry some necessary properties which include biocompatibility, biodegradability and a targeted biodistribution at desired region supplying the therapeutic agents for a long time (Mainardes & Silva, 2004).

A drug can be targeted to a specific tissue in different manners. Passive targeting is that carrier directs the drug to a specific tissue via its main properties, such as size or lipophilicity. When passive targeting is combined with the property of nanocarriers which is being in small size, it provides drugs or nanocarriers to penetrate into tumor region and accumulate in this region in which vasculature is disrupted and is leaky (Figure 1.1) (Lembo & Cavalli, 2010). Active targeting is a targeting mechanism in which drugs or carriers are targeted to particular cell types via recognitions of cell specific proteins by ligands or molecules bound to these drugs or carriers. Physical targeting means that drugs and carrier systems are distributed by external influences, such as magnetic field or heat (Neuberger, Schöpf, Hofmann, Hofmann, & von Rechenberg, 2005)

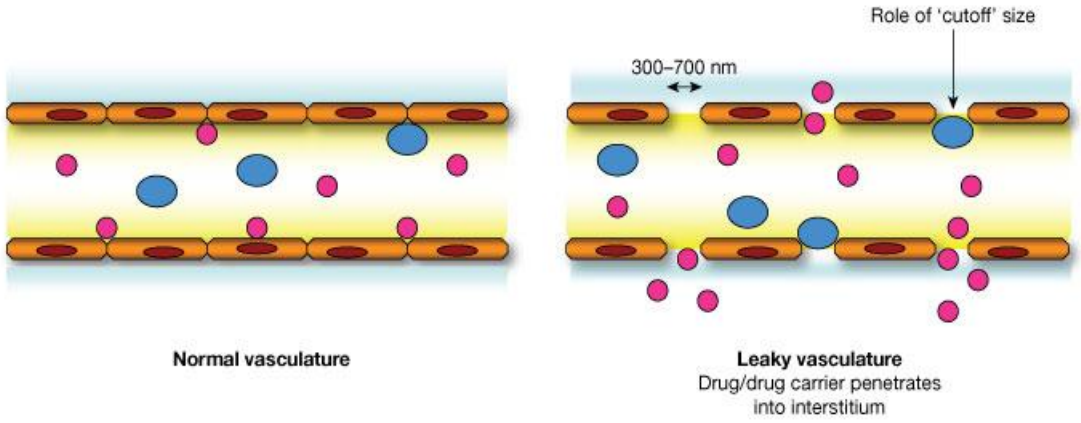

Figure 1.1: Drug delivery systems for cancer treatment (Lembo & Cavalli, 2010).

In many different size and structures, nano drug delivery systems offer techniques to direct and release large amount therapeutic compounds in specific regions. New developments in surface modification and production methods make nanoparticles to get attentions in drug delivery technology. Many different types of these nanostructures such as simple metal core or complex lipid-polymer constructions become functional in many ways to work as drug carriers for diversity of situations (Willis, 2004).

1.6 Magnetic Nanoparticles

Magnetic nanoparticles (MNPs) as their name implies are in nanoscale size and can be manipulated by an external magnetic field. Iron oxide (Fe_3O_4) MNPs around 20 nm in

size are defined as superparamagnetic. Because superparamagnetic particles such as Fe_3O_4 are magnetized under magnetic field and they lose any magnetism in the absence of magnetic field, they get many attentions on their applications for biomedicine (Berry & Curtis, 2003).

1.6.1 Biomedical Applications of Magnetic Nanoparticles

For diagnostic purposes, MNPs have been used in *in vivo* for decades. MNPs are involved in many different biomedical applications due to their distinctive properties that include low toxicity, magnetic behavior and small size (Berry & Curtis, 2003). MNPs have been applied in magnetic resonance imaging (MRI) for diagnosis of diseases, in targeted therapy (hyperthermia) and in drug delivery (Figure 1.2) (Umut, 2013).

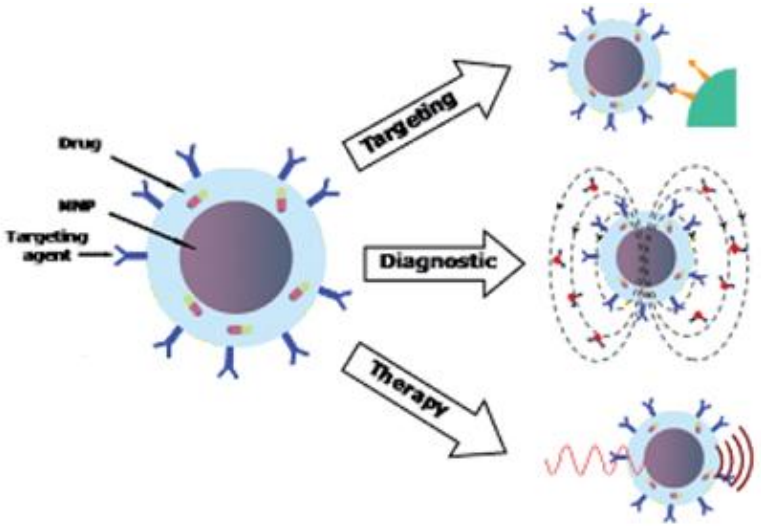

Figure 1.2: Biomedical applications of magnetic nanoparticles (Umut, 2013).

MRI has been used to differentiate one tissue from another tissue through high resolution contrast. MRI systems use contrast agents to increase their diagnostic purposes. Due to their 3–10 nm sizes, paramagnetic ion chelates and ferromagnetic or superparamagnetic nanoparticles have been used as MR contrast agents in clinical diagnosis (Ito, Shinkai, Honda, & Kobayashi, 2005).

In magnetic hyperthermia, MNPs are given to cancer patient and are directed and easily delivered to tumor tissue by application of external magnetic field. Magnetized MNPs in tumor region lose their magnetic energy as heat by changing external magnetic field. This magnetic energy loss in form of heat increases the temperature in tumor tissue and as a result cause cancer cells to die (Gkanas, 2013).

In magnetic targeting, a chemotherapy agent is loaded to a magnetic MNP. Then, drug-bound MNPs are given to the body, and accumulated in the desired region by application of an external magnetic field. In the targeted region, drugs separate from MNPs or cause a local effect (Arruebo, Fernández-pacheco, Ibarra, & Santamaría, 2007).

1.6.2 Magnetic Nanoparticles for Drug Delivery

MNPs have become popular in drug delivery systems because these particles are targeted by magnetic field, which is physical targeting. Therapeutic agents that are delivered to the specific area are either bound to the surface of MNPs or encapsulated by the magnetic nanoparticulate carriers. These agent-loaded MNPs aggregate at the particular desired site by application of an external magnetic field (Figure 1.3) (Mody *et. al*, 2013). Drug can be released from MNPs by simple diffusion or by mechanisms that involve enzymatic activity or by changes of physiological conditions such as pH,

osmolarity, or temperature. Also, release of drug from the drug-linked MNPs can occur magnetically (Arruebo *et. al*, 2007).

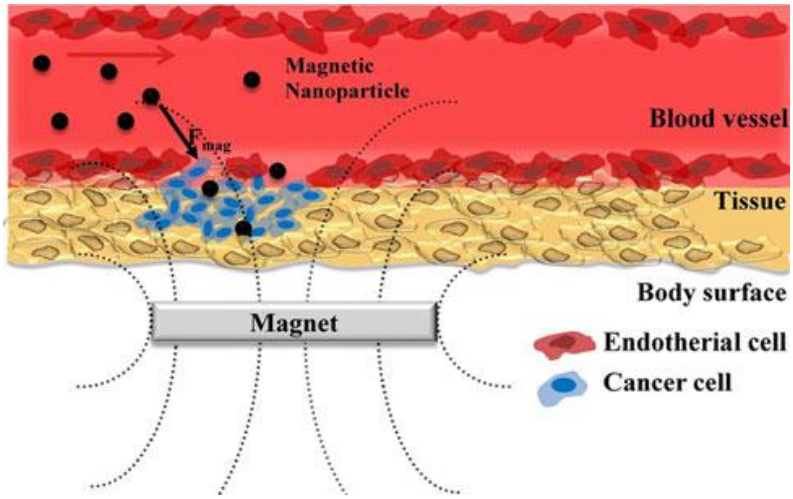

Figure 1.3: Schematic representation of Magnetic drug delivery system under the influence of external magnetic field (Mody *et. al*, 2013).

1.6.3 Structure of Magnetic Nanoparticles

MNPs possess many important structures for different applications of biomedicine. Although they have different structures, all MNPs have to own some fundamental properties to function as DDS. Moreover, these particles need to have enough magnetic properties to accumulate at the desired cells in the presence of a magnetic force. Also, the architecture of MNPs needs to be compatible enough with biological entity to apply to living cells or organisms. MNPs have structure in which a magnetic core is composed of magnetite (Fe_3O_4) or maghemite (Fe_2O_3) and synthetic polymers protect MNPs and make them biologically functional by coating the magnetic core. Sometimes,

for drugs or gene vectors to attach the MNPs, they are bound with specific organic linkers (Figure 1.4) (Pereyra & Claudia, 2013).

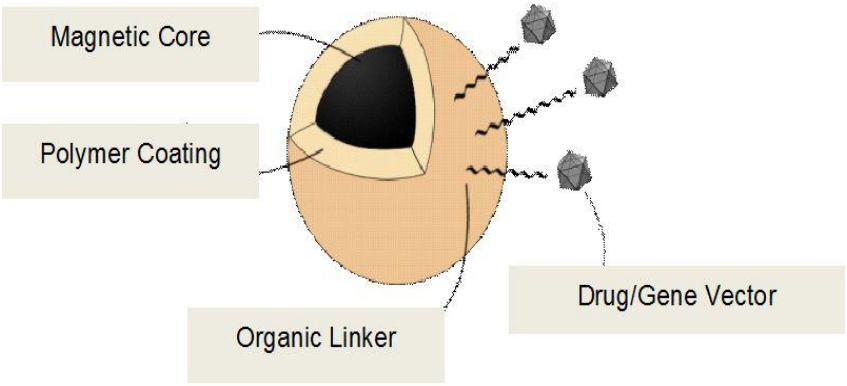

Figure 1.4: General structure of a magnetic nanoparticle (Pereyra & Claudia, 2013).

1.6.4 Polyethylene Glycol (PEG) in Drug Delivery

Polyethylene glycol (PEG) has been a good choice for many years as a drug carrier because it is biocompatible, least toxic and antigenic and high soluble in common solvents or in water. Numerous agents and biological materials like proteins and enzymes have been link to the ends of PEG chains and they can stay biological and enzymatic active (Won, Chu, & Lee, 1998). The structure of PEG is given in Figure 1.5.

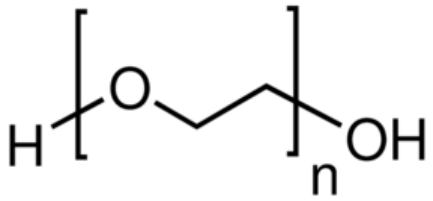

Figure 1.5: Structure of polyethylene glycol (Sigma-Aldrich, n.d.)

Phagocytes eliminate microparticulate carriers from the circulatory system by opsonization, and surface modification of these carriers with PEG delays opsonization. Also, PEG decreases the accumulation of microparticulate carriers by reticuloendotelial system (RES). These 100-200 nm drug carriers with long circulation time efficiently accumulate at tumor sites due to the enhanced permeability and retention effect (Torchilin, 2001).

PEG also has an important role to functionalize the surface groups of dendrimers. As a result, addition of PEG to dendrimers not only increases the water solubility of them but also limits their immunogenicity. Moreover, PEG prevents derivatives of PEGylated dendrimer in the biological condition by increasing their time spent in circulation, which is vital feature for drug delivery systems. Also, PEG coating improves solubility of hydrophobic compounds (Sideratou, Kontoyianni, Drossopoulou, & Paleos, 2010).

To function as delivery systems, multifunctional MNPs need to be designed carefully with important properties. Their surface would protect them from the rapid elimination by the RES after intravenous administration. They need to have drug-loading capacity without changing the physical features of the MNP architecture or magnetization property of the core material, and ability to conjugate MNPs to a targeting ligand or antibody. PEG can meet the requirements above for multifunction of MNPs by coating them (Yallapu, Foy, Jain, & Labhasetwar, 2010).

1.6.5 Folic Acid Directed Drug Delivery

Folic acid is a form of vitamin B9. Folic acid is important to synthesize nucleic acids (DNA and RNA). Folic acid is also vital for rapid cell division and growth and for production of healthy red blood cells. Consuming enough folic acid during pregnancy could prevent major birth defects (Medical News Today, 2013). The structure of folic acid is given in Figure 1.6.

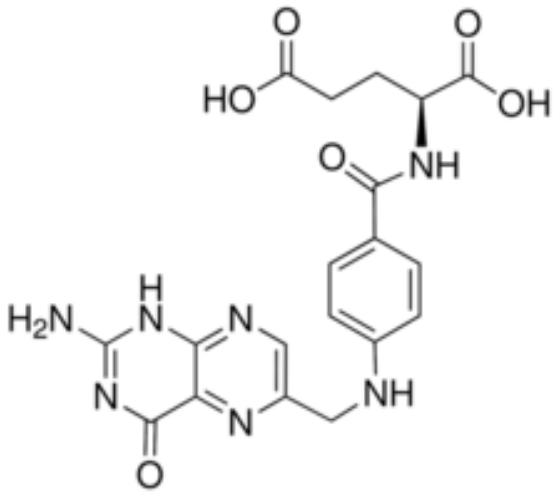

Figure 1.6: Structure of folic acid (Sigma-Aldrich, n.d.-a).

Folic acid targets to the folate receptor which is a cell surface receptor. This folate receptor is overexpressed by many different cancer cells while healthy cells have low expression of folate receptor. Such tumors with overexpressed folate receptors are epithelial, ovarian, cervical, breast, lung, kidney, colorectal, and brain tumors. Folic acid is a non-immunogenic and inexpensive molecule and also it can retain its stability

over large scale of temperatures and wide range of pH values. Conjugation of folic acid to drug carrier does not affect the ability of folic acid to interact with the folate receptor. Binding of folic acid to its receptor causes endocytic internalization of the carrier (Figure 1.7). Drop of the endosomal pH to five triggers dissociation of the folate from its receptor and then, causes release of the drug (Zwicke, Mansoori, & Jeffery, 2012). As a result, these properties of folic acid make it very useful targeting molecule for application of targeted drug delivery system in cancer.

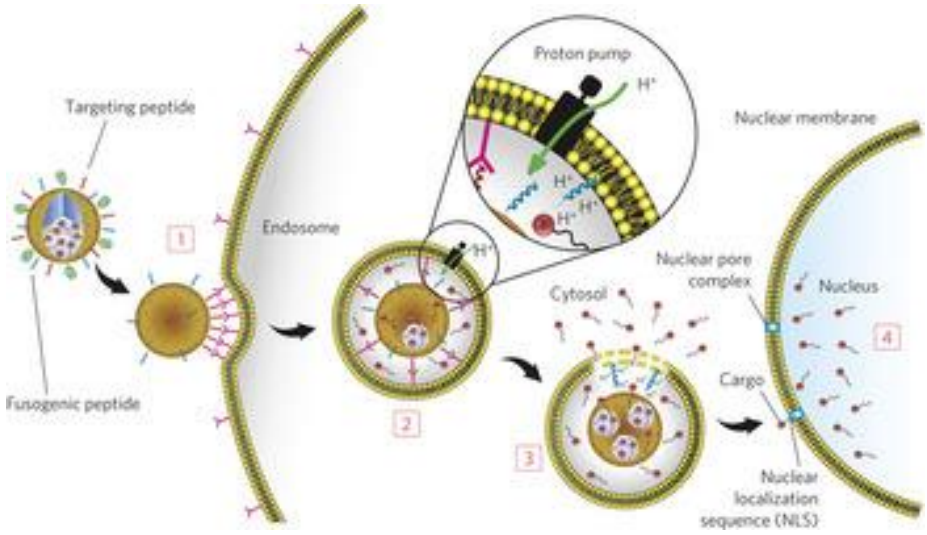

Figure 1.7: Representative picture of the folate receptor-mediated endocytosis pathway (Ashley *et. al*, 2011).

1.7 Synthesis Methods of Magnetic Nanoparticles

There are many effective synthesis methods for production of MNPs with desired size, high stability, and unique dispersion. Co-precipitation, thermal decomposition, microemulsion and hydrothermal synthesis techniques are used to synthesize high-

quality magnetic nanoparticles. These four methods have advantages and drawbacks (Table 1.1). The simplest and more preferred method is co-precipitation technique to synthesize MNPs. Thermal decomposition method provides control on size and morphology of the nanoparticles. Monodispersed MNPs with diverse morphologies can also be synthesized via microemulsion. Disadvantage of this method is consumption of solvent in excess amount. Hydrothermal synthesis method is an infrequently used method to produce magnetic nanoparticles; however, magnetic nanoparticles with high-quality are synthesized via this method. Until now, most studies are conducted on magnetic nanoparticles that have been synthesized by using thermal decomposition and co-precipitation. By these two methods, they are produced in large amounts (Lu, Salabas, & Schüth, 2007).

Table 1.1: Comperassion of MNP Synthesis Methods (Lu et al., 2007)

Synthetic Method	**Synthesis**	**Reaction Temp. (^{o}C)**	**Reaction Period**	**Solvent**	**Surface-Capping Agent**	**Size Distribution**	**Shape Control**	**Yield**
Co-precipitation	Very simple,ambient conditions	20-90	Minutes	Water	Needed, added during or after reaction	Relatively narrow	Not good	High/scalable
Thermal Decomposition	Complicated, inert atmosphere	100-320	Hours-days	Organic compound	Needed, added during reaction	Very narrow	Very good	High/scalable
Microemulsion	Complicated, ambient conditions	20-50	Hours	Organic compound	Needed, added during reaction	Relatively narrow	Good	Low
Hydrothermal Synthesis	Simple, high pressure	220	Hours ca.day	Water-ethanol	Needed, added during reaction	Very narrow	Very good	medium

1.8 Objective of the Study

The objectives of this study can be summarized as follows:

- To synthesize Fe_3O_4 magnetic nanoparticles by thermal decomposition.
- To cover MNP with polyethylene glycol (PEG) monooleate
- To conjugate folic acid to PEG modified MNP.
- To characterize the synthesized MNPs, PEG coated MNP and FA conjugated PEG coated MNP.
- To investigate doxorubicin-loading on folic acid conjugated PEG coated MNPs and doxorubicin release from them.
- To visualize the internalization of magnetic nanoparticles by HeLa cells.
- To investigate cytotoxicities of FA conjugated PEG coated MNPs and Doxorubicin loaded form of them to sensitive and drug resistant lines of HeLa cervical cancer cells.

CHAPTER 2

MATERIALS AND METHODS

2.1 Materials for Magnetic Nanoparticle Synthesis

Iron(III) acetylacetonate ($Fe(acac)_3$), oleic acid, oleylamine, polyethylene monooleate (PEG), folic acid, dicyclohexyl carbodiimide (DCC) and dimethylsulfoxide (DMSO) were purchased from Sigma-Aldrich (U.S.A.). Nitrogen gas was obtained from Asya Gaz (Turkey).

2.2 Synthesis of Magnetic Nanoparticles

In literature, there are many methods including co-precipitation, thermal decomposition and reduction, micelle synthesis, hydrothermal synthesis, and laser pyrolysis techniques synthesize high-quality magnetic nanoparticles (Lu *et. al*, 2007).

In this research, thermal decomposition method was used to synthesize Fe_3O_4 magnetic nanoparticles. Generally, the thermal decomposition is decomposition of iron precursor in a high-boiling temperature stabilizing surfactant solvents such as trioctylamine, oleic acid, oleylamine and so on (Zhao, Zhang, & Feng, 2012). However, the synthesized magnetic nanoparticles have hydrophobic surfactant on their surface, so the magnetic nanoparticles are soluble in hydrophobic solution such as hexane and ethanol.

In this study, Fe_3O_4 magnetic nanoparticles were prepared by the thermal decomposition of $Fe(acac)_3$ in oleic acid and oleylamine solution at 300^0C (Maity,

Choo, Yi, Ding, & Xue, 2009). $Fe(acac)_3$ was dissolved in the mixture of oleic acid and oleylamine, and then mechanically stirred under a flow of nitrogen. The solution was dehydrated at 120^0C for 1h, and then quickly heated to 300^0C and kept at this temperature for 1h. Heat source was removed to cool the black solution. Ethanol was added to the black solution and magnetic nanoparticles were precipitated by magnet. The nanoparticles were washed several times with ethanol. The synthesized Fe_3O_4 magnetic nanoparticles (OL-Fe_3O_4) which have oleic acid and oleylamine on their surface were labeled as MNPs.

2.3 Synthesis of PEG Coated Magnetic Nanoparticles

MNP has hydrophobic property due to the hydrophobic surfactants (oleic acid and oleylamine) on the surface of Fe_3O_4 particles. To be biocompatible, soluble in hydrophobic environment and able to carry drug, the magnetic nanoparticles should be coated with an appropriate polymer or dendrimer.

In this research, OL-Fe_3O_4 magnetic nanoparticles were mixed with PEG in distilled water and the solution was stirred overnight at room temperature. Then, PEG coated MNP (PEG-MNP) was precipitated by magnet. The nanoparticles were washed with distilled water until clear supernatant was observed.

2.4 Folic Acid Modification of PEG-MNP

PEG-MNP was modifed with activated folic acid (Zhang, Rana, Srivastava, & Misra, 2008). Folic acid (FA) is dissolved in dimethyl sulfoxide (DMSO). Dicyclohexyl carbodiimide (DCC) is added to the solution and the solution is stirred for 2 h in a

nitrogen atmosphere. Then, PEG-MNP is added and continuously stirred for 2 h in a nitrogen atmosphere. Finally, FA modified PEG-MNP (FA-MNP) was washed twice with distilled water and stored in distilled water at room temperature.

2.5 Drug Loading

In this study, the absorptions of the different concentrations of doxorubicin (Dox) were measured to determine the standard curve of its absorption versus concentration. Standard curve were used to measure concentration of Dox remaining in solution after Dox loading to FA-MNP.

Different concentrations of Dox were added to the eppendorf tubes containing same amount of FA-MNP. The tubes were placed to the rotary shaker (Biosan Multi RS-60 Rotator). Then, the tubes were shaked at room temperature for 24 hours. Dox loaded FA-MNP was precipitated by application of magnet. Then, supernatant was collected and absorption of supernatant was measured to determine the remained Dox concentration.

2.6 Drug Release

After drug loading process, drug-loaded FA-MNPs in eppendorf tubes are washed with distilled water and same amount of acetate buffers with pH 4.13 and 5.14, and pH 7.4 added to the tube. Then, it is placed to rotator shaker. After 3 hours, particles are precipitated by magnet and supernatant is taken to new tube for measurement of drug absorbance. After that, the solvents were added to the tube and the tubes were rotated. This process was repeated several times for 72 h. Finally, concentration of released drug

is calculated from its absorbance at 480 nm measured by a UV spectrophotometer (Multiskan GO, Thermo Scientific) via the slope of standard curve.

2.7 Cell Culture

2.7.1 Cell Line and Culture Condition

Parental sensitive HeLa and doxorubicin resistant HeLa (HeLa/Dox) cells were cultured in RPMI 1640 medium (Thermo Scientific, USA) with 10% heat inactivated fetal bovine serum (FBS) (Biochrome, Germany) and 0.2% gentamycin (Biological Industries, Israil). Incubation condition of cells in a Heraeus incubator (Hanau, Germany) involved 37^{o}C, a humidified atmosphere with 5% CO_2.

2.7.2 Subculturing

Subculturing is applied to cells that have 80% cell confuency in a flask to prevent them from dying before all nutrients in the medium are consumed. Firstly, old medium is taken from the flask and cells are washed with 5 ml phosphate buffered saline (PBS) for T-75 filter capped tissue culture flask. It is important that washing the cells with PBS prevents trypsin from inhibiton caused by medium and waste products. Secondly, 1 mL trypsiın was added to the flask and the flask is put into the incubator with 37^{o}C, 5% CO_2, humidified condition for a few minutes. During incubation, trypsin detachs cells from the surface of the flask via digestive enzymatic activity. Thirdly, 5 ml medium supplemented with serum is added to flask for inhibition of trypsin and used to homogenize cells by pipetting. Cell suspension is transferred to 15 mL Falcon tube (Greiner) and centrifuged at 1000 rpm for 5 minutes. Supernatant is discarded and 3 mL fresh medium is added to tube to resuspend the pellet. Then, a proper amount of cell

suspension is transferred to the flask and total volume is completed to 12 mL by medium addition. For HeLa/Dox cells, there is one additional step in which 12 µL of 500 µM doxorubicin solution is added to their medium to maintain resistance. Finally, cells are incubated at 37^{o}C.

2.7.3 Cell Freezing

In a tissue culture flask, when cells reach at least 80% confluence or more, they are trypsinated and detached. The detached cells are resuspended in 4 mL of medium and centrifuged at 1000 rpm for 5 min. Supernatant is discarded and cells are resuspended with 4 ml PBS. Again, the cells are centrifuged at 1000 rpm for 5 min. Supernatant is removed and cells are suspended in 1 mL of cold freezing medium (90% (v/v) complete growth medium supplemented with 10% (v/v) DMSO (Sigma-Aldrich, USA)) to have a final concentration of approximately 2x10^{6} cells per ml. This cell suspension is transferred into the cryovials (Greiner) and maintained at 4ºC for 30 min, then kept in -20ºC for 3-4 hours before the overnight incubation at -80ºC. Finally cryovials are transferred to liquid nitrogen container for long term storage.

2.7.4 Cell Thawing

The cryovials containing the frozen cells are taken from liquid nitrogen container and immediately placed into a 37°C water bath. Quickly after cells are thawed, they are transferred to a falcon tube and 4 mL pre-warmed growth medium is added on the thawed cells. Then, cell suspension is centrifuged at 1000 rpm for 5 min. Supernatant is discarded. The cells are gently resuspended in growth medium, and transferred into a cell culture flask. Finally, cell containing flask is incubated at 37^{o}C.

2.7.5 Cell Counting

Trypan blue and a hemocytometer as a microscope slide are used for viable cell counting. Trypan blue is applied to distinguish viable cells from dead cells. This means that trypan blue dye selectively penetrates membranes of the dead cells and colors them blue while cell membranes exclude viable cells from trypan blue staining and alive cells are not stained. In this method, 225 μL of the cell suspension to be counted is mixed with 25 μL trypan blue in an eppendorf tube. The shoulders of the hemocytometer are moisturized and the coverslip is affixed on them. Some cell suspension containing trypan blue is loaded to the chamber of hemocytometer at the edge of the cover slide. The grid lines of the haemocytometer are focused under light microscope. The number of cells in the area of 16 squares which is composed of 256 small squares is counted. During cell counting, live cells (unstained with trypan blue) are always counted and stained cells are ignored. Cell suspension to be used for an experiment must have more than 90 % live cells of total cell number. Otherwise, cell suspension cannot be used for any experiment. Cell number in 1 mL cell suspension is calculated by following formula:

$$\text{Cell number/mL} = \frac{\text{Number of cells counted on 16 squares}}{256} \times 4 \times 10^6$$

2.8 Internalization of Nanoparticles

Internalization of nanoparticles by HeLa cells was investigated by Purssian blue staining (Sigma-Aldrich) and/or using fluorescent property of doxorubicin loaded to FA-MNP.

2.8.1 Detection of Internalized Nanoparticles by Purssian Blue Staining

Iron oxide nanoparticles was stained by purssian blue staining method (Boutry *et. al*, 2009). The nanoparticles that were internalized by HeLa cells were detected by this technique. This method provides two solutions, working iron solution and working pararosaline solution. To prepare working iron stain solution, potassium ferrocynanide solution and HCl (1:1 v/v) are mixed in a falcon tube. For preparation of working pararosaline solution, pararosaline solution is added to dH_2O to be 2% (v/v) in a falcon tube. Acid ferrocyanide in working iron stain solution reacts with iron causing production of blue color or dark blue in case of heavy deposit of iron, while working pararosaline solution stains cell producing red color in nucleus and pink color in cytoplasm.

Procedure of purssian blue staining is modified. Firstly, cover slides were placed inside the wells of 6-well plate. 200000 cells were seeded to each well. Old medium was removed after 24 hours and cells were washed with PBS solution. 2mL fresh media containing different concentration of Fe_3O_4 particles were added to wells. Cells were incubated at 37^oC and 5% CO_2 for 7 hours. Then, cells were washed 5 times with PBS to get rid of MNPs that has not been internalized by cells. Working pararosaline solution is added on cells in wells and cells are incubated for 10 minutes. The cells are washed one time with distilled water. Working pararosaline solution is added on cells in the flask and the flask is incubated for 5 minutes. The cells are washed one time with distilled water and left to dry. Finally, the cells are observed under light microscopy and photographed.

2.8.2 Detection of Internalized Nanoparticles by Fluorescent Microscopy

Doxorubicin is a chemotherapy drug and has a fluorescent property. When it is loaded to FA-MNPs, they gain fluorescent property and can be detected by fluorescent microscopy.

Firstly, 200000 cells were seeded to each well of 6-well plate. Old medium was removed after 24 hours and cells were washed with PBS solution. Then, 2mL fresh media containing different concentrations of Dox loaded MNPs were added to wells. Cells were incubated at 37^{o}C and 5% CO_2 for 7 hours. Then, cells were washed 5 times with PBS to get rid of the magnetic nanoparticles that have not been internalized by cells. The cells are observed under fluorescent microscope and photographed.

2.8.3 Cell Proliferation Assay

XTT cell proliferation assay is a colorimetric assay for quantification of cell proliferation, viability, and cytotoxicity of a drug. In this assay, XTT reagent (a tetrazolium salt) is reduced to formazan by the mitochondrial enzymes in live cells.

50 μL cell suspension were added to the wells of 96 well plate (Figure 2.1) and incubated at 37^{o}C and 5% CO_2 humidified atmosphere for 24 h. After the incubation, medium is discarded and cells were washed with PBS.

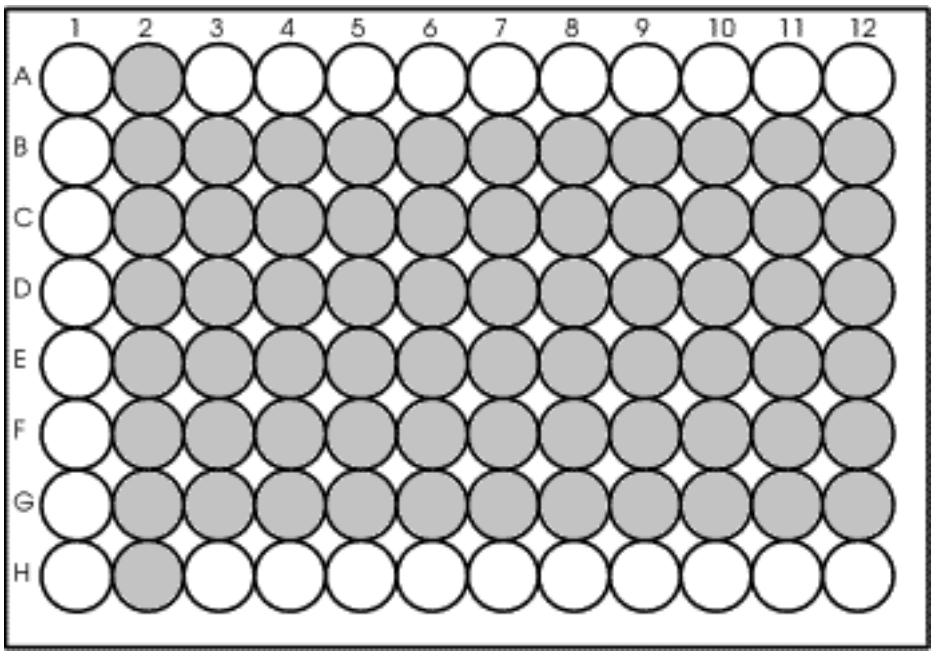

Figure 2.1: Representative picture of cell seeded 98 well plate. Gray wells represent cell seeded ones.

Then, 200 µL of highest drug dose (HDD) containing medium (10 µM doxorubicin for HeLa or 1000 µg/mL nanoparticles for HeLa and HeLa/Dox) is added to each wells of 3rd column and 50 µL fresh medium is added to remaining wells. 150 µL of HDD containing medium were transferred from 3rd column to 4th column and mixed well with 50 µL medium in each wells of 4th column. 150 µL of drug containing medium were transferred from 4th column to 5th column and mixed well with 50 µL medium in each wells of 5th column. This dilution was continued till 12th column (Figure 2.2). 50 µL medium was added to all wells of the plate, so HDD became half of the strating concentration (5 µM doxorubicin for HeLa or 500 µg/mL nanoparticles for HeLa and HeLa/Dox). The plate was incubated at 37^{o}C and 5% CO_2 humidified atmosphere for 72 h. After that, 50 µL activated XTT is added to each wells and incubated for 4 h. Absorption of samples in wells was measured at 492 nm. 1st column was medium

control and 2nd column was cell control. To find out the absorbance of only cells, absorbance of 1st column was subtracted from absorbance of 2nd column. This absorbance of cells was accepted as 100% proliferation. Absorbance of drug treated cells in column 3-12 were calculated by subtracting average absorbance of A and H wells from that of cell seeded wells in same column. Percentage of cell proliferation was calculated by dividing absorbance of column to that of control.

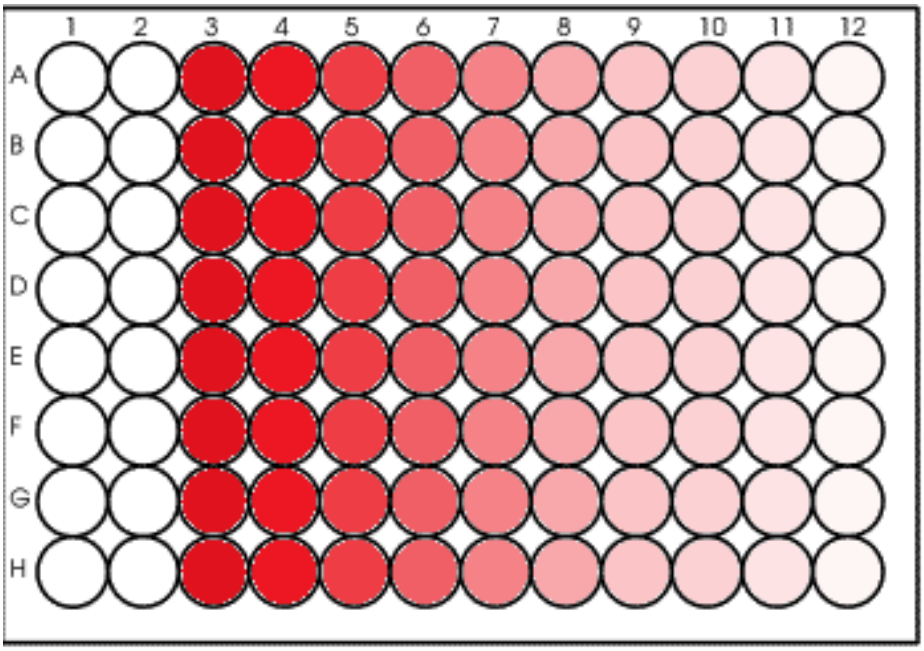

Figure 2.2: Representative picture of drug dilution in 96 well plate.

2.9 Statistical analysis

Results gathered from at least two independent experiments are expressed as mean ± SEM and were analyzed using GraphPad Prism Version 5.01 (GraphPad Inc., USA)

with one-way ANOVA followed by Tukey's Multiple Comparison Test. Resullts were significant when $p<0.05$.

CHAPTER 3

RESULTS AND DISCUSSION

3.1 Chemical Characterization

Oleic acid and oleylamine on their surfaces make the synthesized MNPs hydrophobic beause they are produced by decomposition of $Fe(acac)_3$ in mixture of these two surfactants in high temperature. Then, the synthesized magnetic nanoparticles are coated with PEGmonooleate by hydrofobic interaction between hydrofobic surfactants on MNPs and oleate part of PEG monooleate in distilled water which is hydrophilic solvent.

3.1.1 Chemical Characterization of MNPs

Magnetic nanoparticles are synthesized in small size and narrow size range via termal decomposition method. The sizes of magnetic core and morphological properties were observed through TEM images. The chemical groups and chemical interactions involved in synthesized MNPs were identified using the FTIR methods. Crystal structures of synthesized MNPs were analyzed by XRD. The qualitative and quantitative information about the volatile compounds of the nanoparticles have been provided by TGA. Magnetic properties of MNPs were determined through VSM analyses.

3.1.1.1 Transmission Electron Microscopy of MNPs

Size and morphology of synthesized OL-Fe_3O_4 magnetic nanoparticles (MNPs) have been observed by Transmission Electron Microscopy (TEM). Obtained images (Figure 3.1) showed that MNPs are almost spherical and have more uniform size distribution. The average diameter of MNPs is approximately 10 nm. Images of MNPs in two solvents (ethanol and hexane) are taken by TEM. Ethanol can dissolve both hydrophobic and hydrophilic substances because it is a versatile solvent while hexane dissolves only hydrophobic materials due to its hydrophobic property. As a result, MNPs are more dispersed in hexane than in ethanol because MNPs are hydrophobic due to oleic acid and oleylamine on their surface.

a)

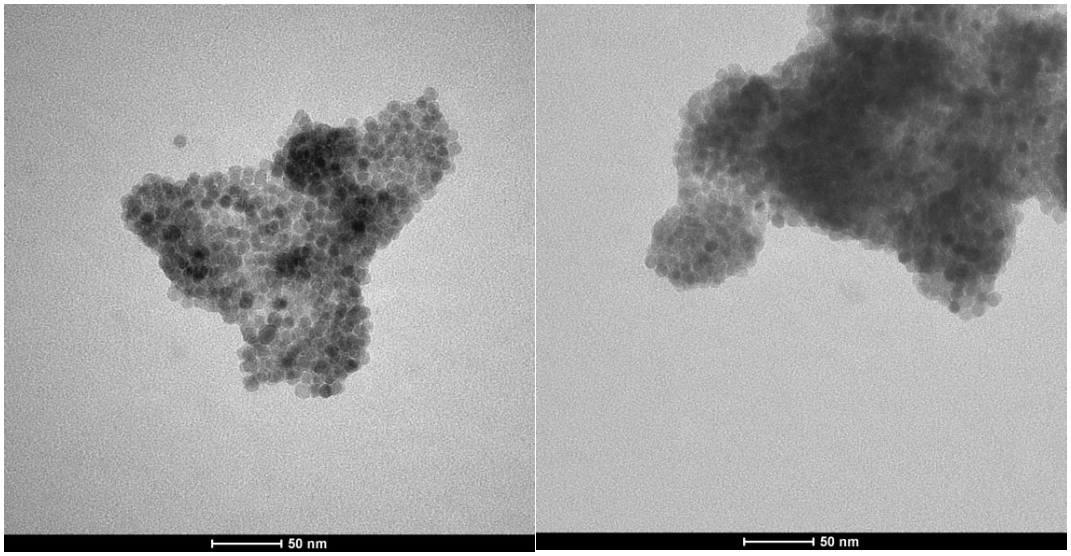

b)

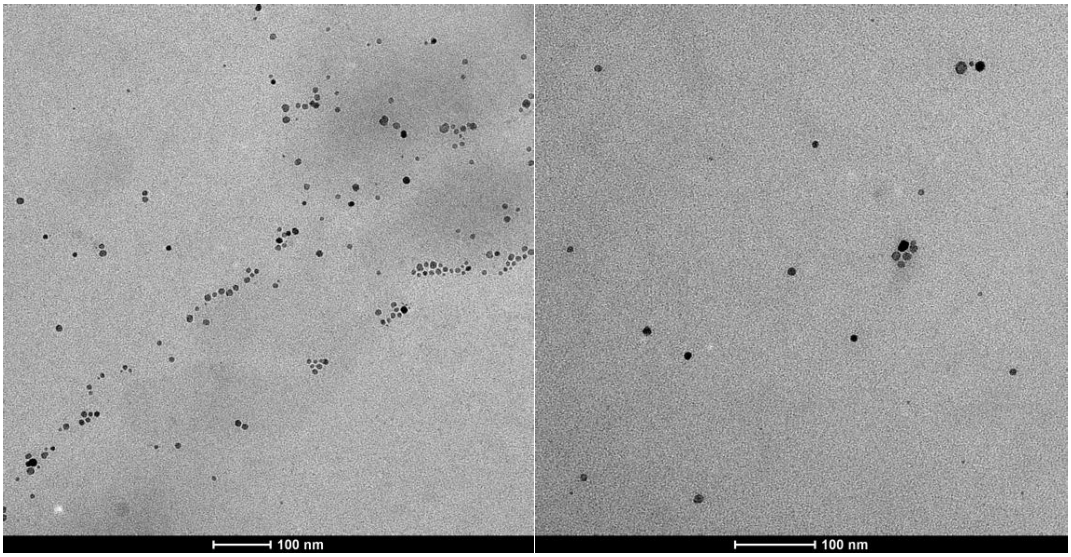

Figure 3.1: TEM images of MNPs (a): in Ethanol, b): in Hexane)

3.1.1.2 X-Ray Diffraction

The crystal structure of sythesized iron oxide (OL-Fe_3O_4) nanoparticles was determined by XRD. Diffraction peaks at 30.25, 35.41, 43.41, 57.30, 62.70 and 74.49 2θ (degrees) which are corresponding to specific diffractive plane indexes (220), (311), (400), (422), (511), (440) and (533) respectively (Figure 3.2). XRD patterns of OL-Fe_3O_4 were examined by comparing to peaks of standard magnetite in JCPDS file (PDF no: 01-075-1609). All peaks are characteristic peaks of the magnetite (Fe_3O_4) crystals that have an inverse cubic spinel structure. XRD results revealed the presence of the Fe_3O_4 crystals in the synthesized nanoparticles OL-Fe_3O_4. The peaks shown in the XRD pattern of the prepared sample are sharp and intense, indicating crystallinity of the sample.

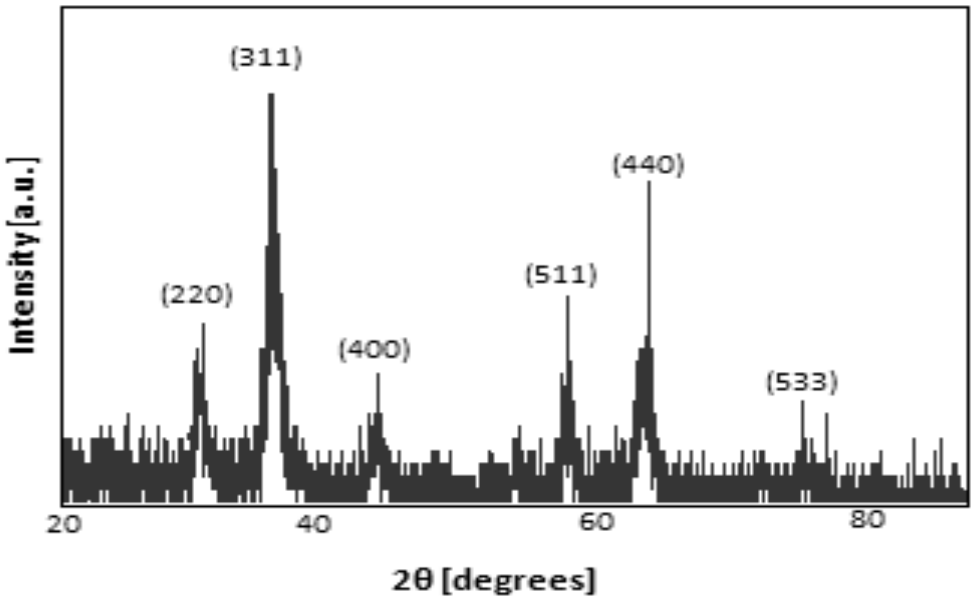

Figure 3.2: X-Ray powder diffraction (XRD) patterns of synthesized iron oxide (OL-Fe_3O_4) nanoparticles.

3.1.1.3 Fourier Transform Infrared Spectroscopy of MNPs

In order to confirm the chemical composition of synthesized nanoparticles, fourier transform infrared spectroscopy analysis were obtained. The peak located in the 583 cm^{-1} region, characteristic for the Fe-O group MNPs' spectra, confirms that the products contain magnetite (Fe_3O_4). All characteristic peaks of OL-Fe_3O_4 were present in Figure 3.3. The band at 580 cm^{-1} corresponded to the vibration of the Fe–O bonds in the crystalline lattice of Fe_3O_4 (Li, Wei, Gao, & Lei, 2005). The bands at 2852 and 2922 cm^{-1} were attributed to the asymmetric CH_2 methylene stretch and the symmetric CH_2 stretch in oleic acid, respectively (Maity *et. al*, 2009). The band at 1409 cm^{-1} corresponded to the CH_3 umbrella mode of oleic acid. The bands at 1427 and 1523 cm^{-1} were attributed to the asymmetric (COO) carboxyl and symmetric (COO) stretch vibration band (Yang, Peng, Wen, & Li, 2010).

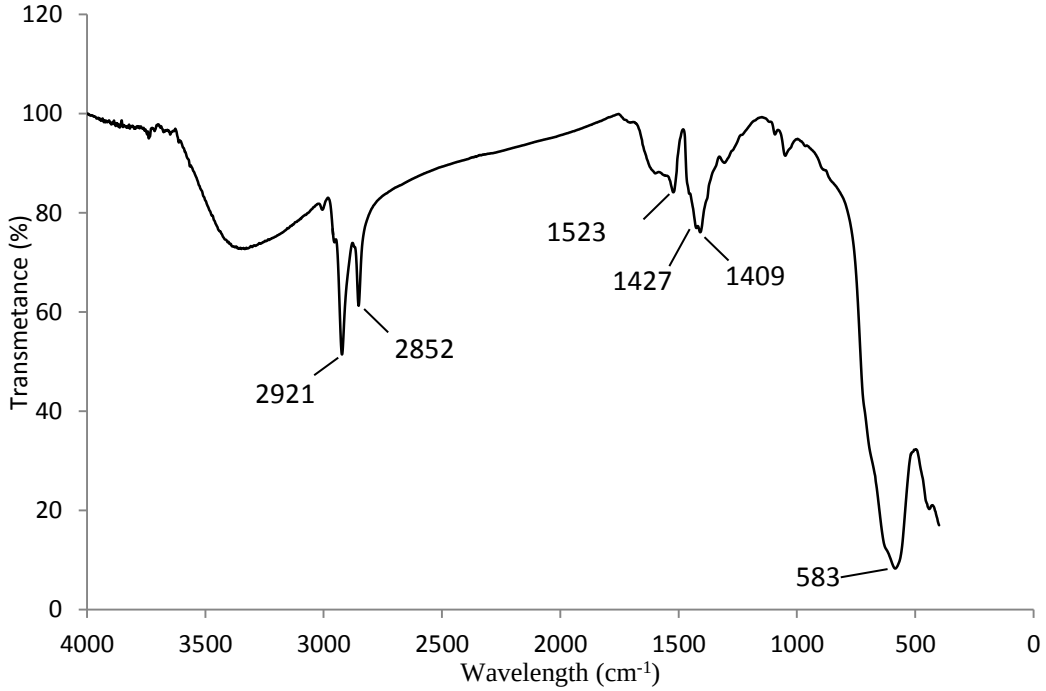

Figure 3.3: FTIR spectrum of MNPs.

3.1.1.4 TGA (Thermal Gravimetric Analysis) of MNPs

The percents of Fe_3O_4 and OL (Oleic acid and Oleylamine) in the nanoparticles were measured by thermo-gravimetric analyzer. The TGA analysis of MNPs (OL-Fe_3O_4) provides qualitative and quantitative information about the volatile components. The TGA analysis of MNPs has two weight loss phases (Figure 3.4). The first weight loss (~2%) belongs to the decomposition of ethanol absorbed by OL molecules on the surface of Fe_3O_4 particles. In the second phase of weight loss which is ~10% of total mass, OL molecules were decomposed by increasing the temperature. TGA result also suggests that MNPs have OL molecules on their surface.

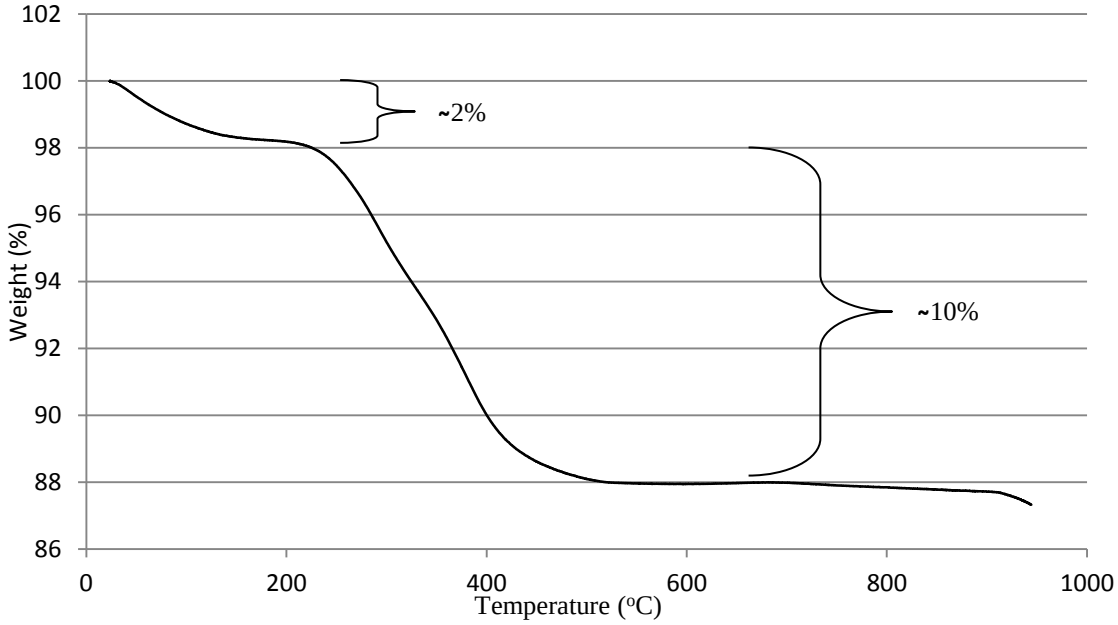

Figure 3.4: Thermal gravimetric analyses of MNPs.

3.1.1.5 VSM (Vibrating Sample Magnetometer)

Magnetic hysteresis curve was obtained by vibrating sample magnetometer. The applied magnetic field was changed and magnetization properties of synthesized OL-Fe_3O_4 nanoparticles were measured at 37˚C. Remanence (magnetization of particles after removal of magnetic field) and coercivity (a measurement of a reverse field needed to drive the magnetization to zero after saturation) were not observed in the hysteresis curve. This phenomenon proved that all nanoparticles synthesized in this study are superparamagnetic. The saturated magnetization (MS) of MNPs is 55 emu/g (Figure 3.5).

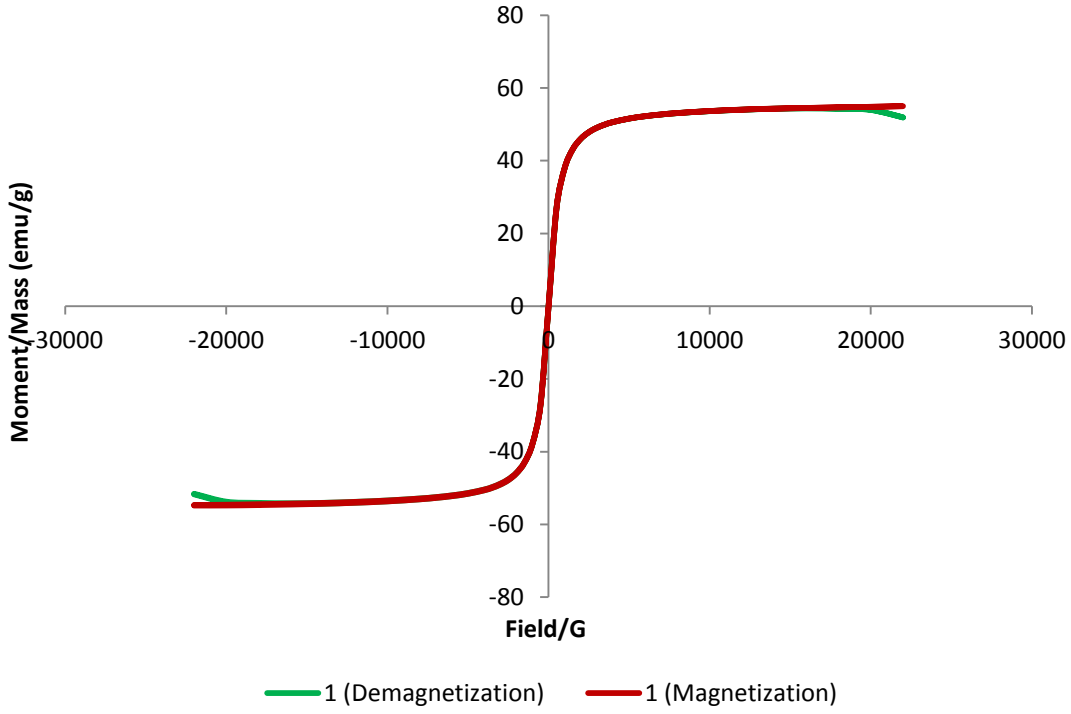

Figure 3.5: Vibrating sample magnetometer (VSM) results show magnetization and demagnetization curves of MNPs (55 emu/g) at 37˚C.

3.1.2 Chemical Characterization of PEG-MNP

The synthesized magnetic nanoparticles are coated with PEG monooleate by hydrofobic interaction between hydrofobic surfactants on MNPs and oleate part of PEG monooleate in distilled water which is hydrophilic solvent.

Sizes and morphologies of PEG-MNPs were analyzed by Transmission Electron Microscopy (TEM) images. The chemical groups and chemical interactions involved in PEG-MNPs were analyzed by using the FTIR methods. The qualitative and quantitative information of nanoparticles have been provided by TGA.

3.1.2.1 TEM Characterization of PEG-MNP

Size and morphology of PEG-MNPs were examined by TEM. TEM results (Figure 3.6) demonstrated that PEG-MNPs had almost spherical and more uniform size distribution. The average diameter of MNPs is approximately 15 nm. Images of PEG-MNPs are taken by TEM.

a)

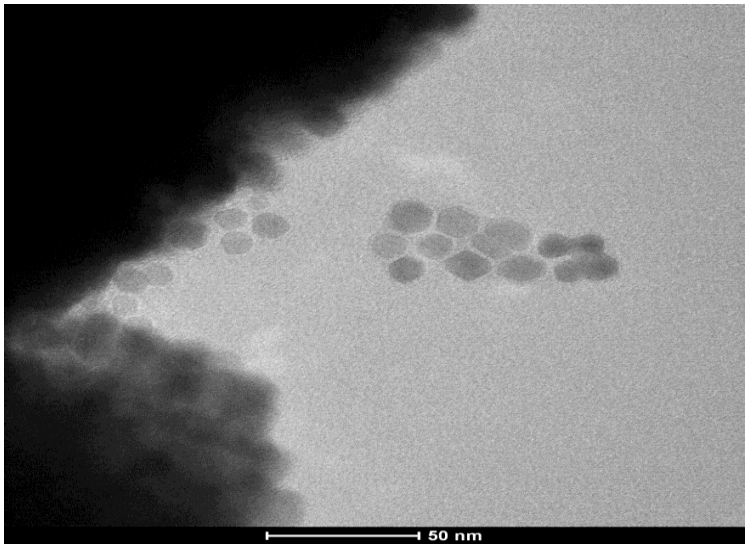

b)

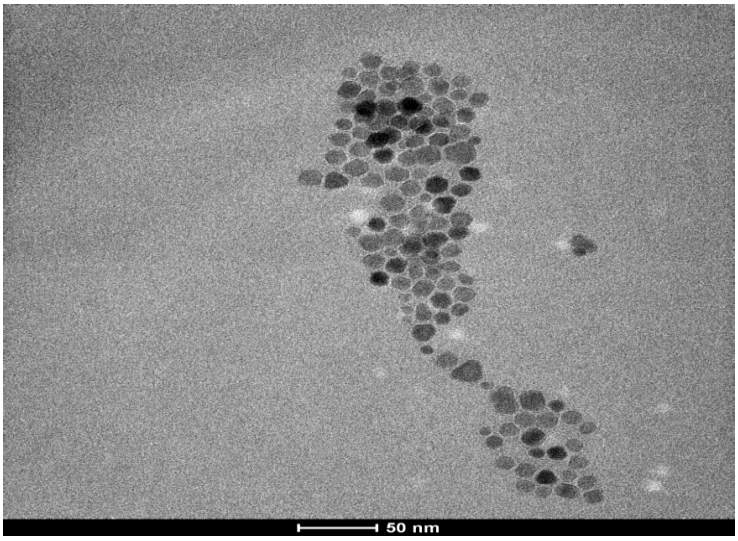

Figure 3.6: TEM images of PEG- MNPs.

3.1.2.2 Fourier Transform Infrared Spectroscopy (FTIR) of PEG-MNP

The FTIR analyses of PEG-MNP were performed to confirm that MNPs were coated with PEGmonooleate. The peaks at 946 cm^{-1} and 1109 cm^{-1} indicated the stretching vibration of functional CH_2 group and the stretching vibration of functional group of C–O of PEG respectively while the absorption band observed at 1735 cm^{-1} was caused by C=O carbonyl group of PEG (Figure 3.7). Thus, these results confirmed that MNPs were successfully coated with PEG.

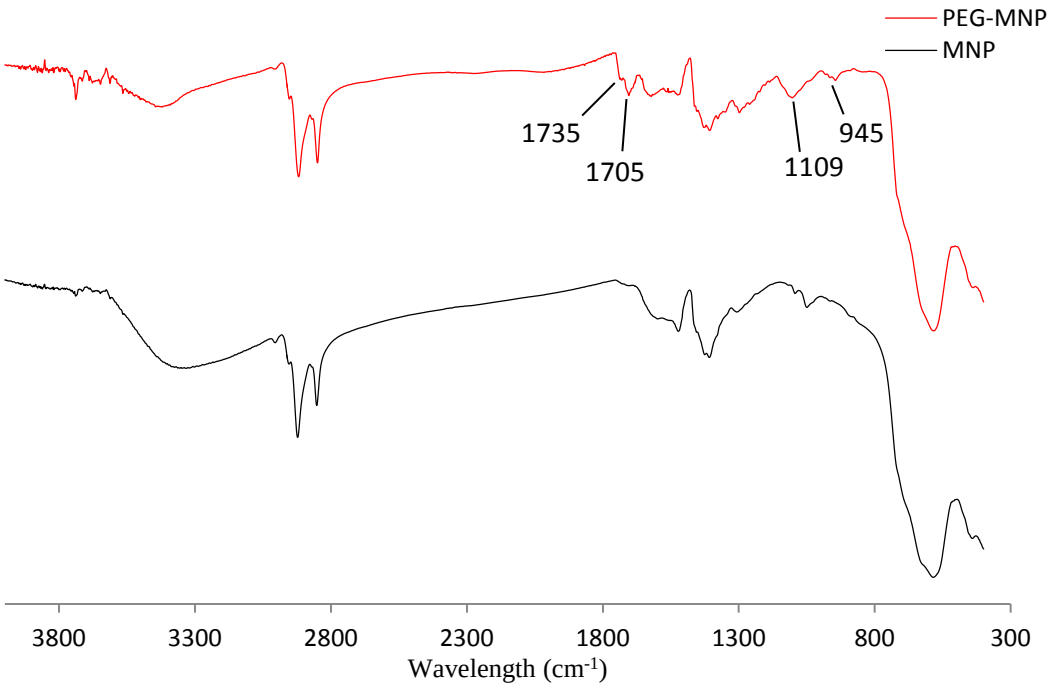

Figure 3.7: FTIR spectrum of PEG-MNPs.

Oleate group of PEG monooleate formed hydrophobic interaction with oleic acid on the surface of MNPs. Thus, this interaction formed interpenetration layer and PEG formed secondary layer by coating MNPs (Figure 3.8). The intense peak at 1705 cm^{-1} was due to the C=O stretching of oleate part of PEG monooleate. This peak was showed at 1710

cm^{-1} for second layer of oleic acid on MNPs by Yan *et. al* (Yang *et. al*, 2010). The FTIR result showed that MNPs were successfully coated with PEG.

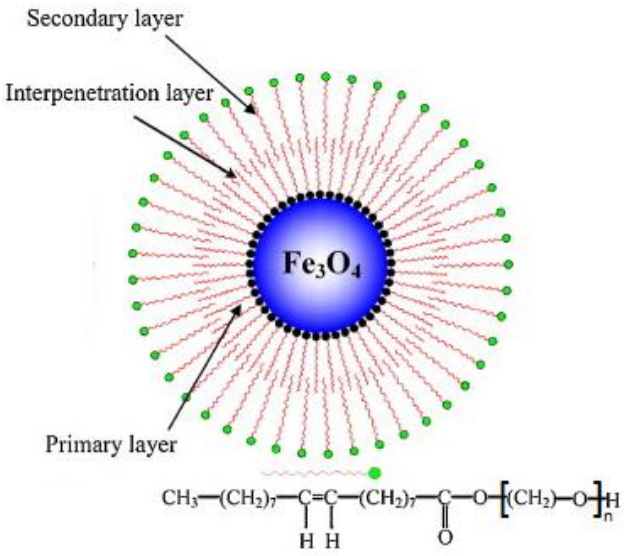

Figure 3.8: Schematic representation of PEG coated MNPs (Yang *et. al*, 2010).

3.1.2.3 Thermal Gravimetric Analysis (TGA)

TGA was used to show existence of PEG on the surface of particles and to determine amount of PEG by decomposition of particles. TGA analysis revealed that MNPs had 12% weight loss due to decomposition of oleic acid and oleylamine while PEG-MNPs had 44% weight loss (Figure 3.9). 32% difference showed that PEG exists on the surface of the nanoparticles.

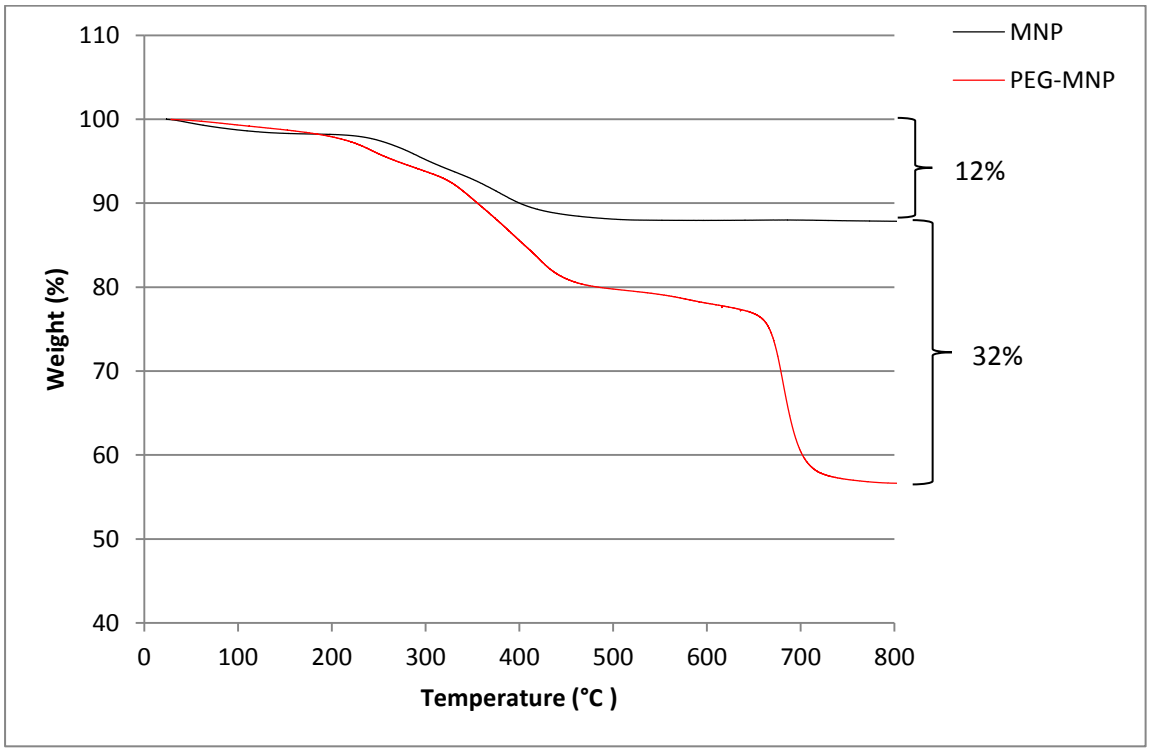

Figure 3.9: Thermal gravimetric analyses of PEG- MNPs.

3.1.3 Chemical Characterization of FA-MNPs

The FTIR analysis was made to demonstrate FA modification of PEG-MNPs.

3.1.3.1 Fourier Transform Infrared Spectroscopy of FA-MNPs

The FTIR result of FA-MNP showed that the characteristic absorption peaks 1433 and 1606 cm^{-1} of FA-MNP (Figure 3.10) were also shared by the FTIR spectrum of FA (Appendix B.2). The characteristic band of 1433 cm^{-1} wavelength was belonging to the phenyl ring of folic acid. 1606 cm^{-1} band indicated $–NH_2$ bending vibration of FA (Keskin, 2012). Because of these bands, modification of PEG-MNPs with FA was successfully achieved.

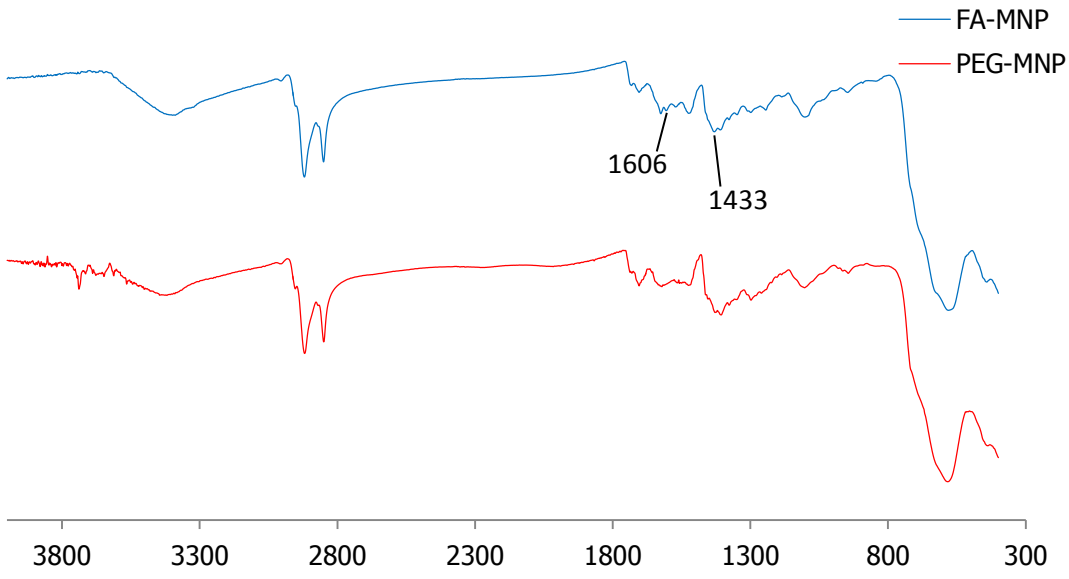

Figure 3.10: FTIR spectrum of FA-MNPs.

3.2 Drug Loading

Different concentrations of doxorubicin were mixed with 500 μg/ml FA-MNPs in Tris buffer having pH 7 by rotary shaker at room temperature for 24 h. Increase in total drug concentration in mixture decreased the percentage of the doxorubicin loaded to FA-MNPs (Figure 3.11). This did not show the concentration of drug loaded to FA-MNPs.

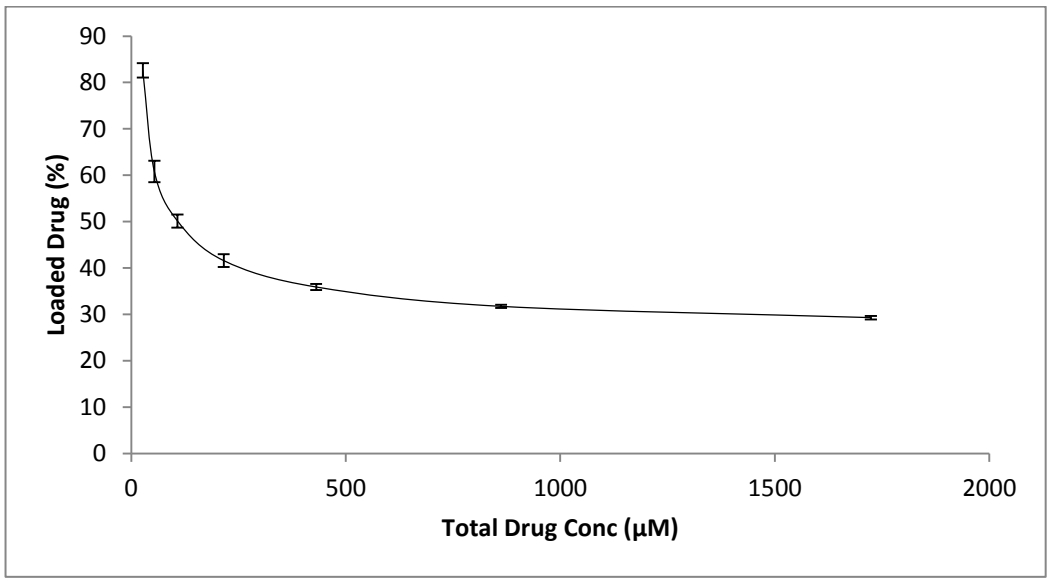

Figure 3.11: Percentages of doxorubicin loaded to FA-MNPs in different concentrations of doxorubicin.

In 1724 μM doxorubicin concentration, ~ 29% of total doxorubicin was loaded to FA-MNPs. This was seen that ~29 % drug loading could be considered as low drug loading capacity of MNPs. However, ~29 % drug loading was equal to around 505 μM doxorubicin loaded to FA-MNPs which was the highest drug concentration in molarity (Table 3.1). Loaded drug concentration of drug was calculated from the absorption by

using standard curve of doxorubicin (Appendix D). However, 78 µg of doxorubicin per mg of nanocomposite was sufficient to kill cancer cells (Chen *et. al*, 2011). In this study, 290 µg of doxorubicin was successfully loaded to 1 mg nanoparticles. FA-MNPs had nearly 50% doxorubicin loading capacity (Zhang *et al.*, 2008), which was higher than that was found in this study. There are some factors that affect the loading capacity of particles. First of all, size of PEG could have role on loading capacity. If the polymer that coats the particles is longer, the particles could have higher drug loading capacity. Also, pH of environment could affect the amount of drug loaded to the particles. Moreover, buffer type used during drug loading could increase or decrease drug loading. Finally, particles used in this study were in dH_2O; in other words, particles were moisture. When dried particles were used for drug loading, more drugs could be loaded as moisture enters between polymers on particles. However, they cannot be as dispersed in a solvent after the particles were dried. This is the reason why the particles were not dried.

Table 3.1: Concentration of doxorubicin loaded to FA-MNPs.

At pH 7	
Total Drug Conc (µM)	**Loaded Drug Conc ± SEM (µM)**
1724	505.01 ± 11.23
862	273.40 ± 5.01
431	154.70 ± 5.06
215.50	89.63 ± 5.24
107.75	54.02 ± 2.65
53.88	32.76 ± 2.17
26.94	22.25 ± 0.71

3.3 Drug Release

The release profiles of doxorubicin from Dox-FA-MNPs in acetate buffer with pH 4.13 and pH 5.14 and pH 7.4 at 37^{o}C were measured at 480 nm in 3 h intervals by UV spectrophotometer. Drug release was investigated at acidic pH to mimic the endosomal condition. Moreover, the release temperature was 37^{o}C which is equal to body temperature and also incubation temperature of cells. According to the results, at low pH 4.13, drug release from nanoparticles occurred faster and higher than at two other pH values (Figure 3.12). Acidity of environment affected the release of doxorubicin *in vitro* and the more the acidic condition, the more release rate of doxorubicin when compared two different pH values. Percentages of drug releases from Dox-FA-MNPs were 15.74 %, 14.27 % and 10.01 % in acetate buffers with pH 4.13, pH 5.14 and pH 7.4 respectively in 72 h.

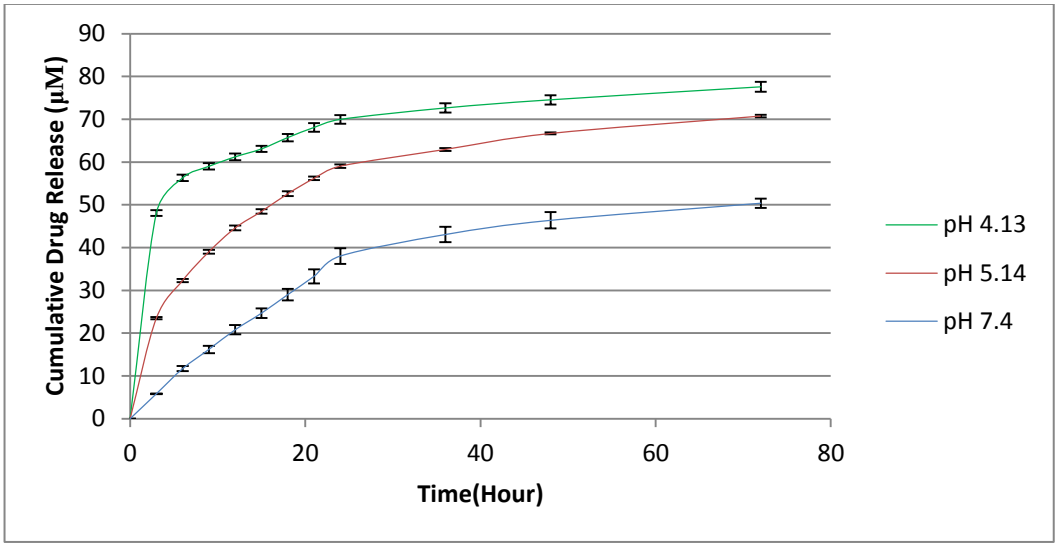

Figure 3.12: Released doxorubicin concentration from Dox-FA-MNPs in acetate buffers with different pH values.

Table 3.2: Concentration of released doxorubicin from Dox-FA-MNPs in different solution and different pH Values.

	pH 4.13	pH 5.14		pH 7.4	
Time (h)	Drug Conc ± SEM (μM)	Drug Conc ± SEM (μM)		Drug Conc ± SEM (μM)	
0	0.00	0.00	0.00	0.00	0.00
3	48.09 ± 0.68	23.51 ± 0.28		5.83 ± 0.05	
6	56.28 ± 0.74	32.31 ± 0.39		11.70 ± 0.61	
9	58.99 ± 0.73	39.02 ± 0.47		16.21 ± 0.86	
12	61.21 ± 0.78	44.60 ± 0.53		20.80 ± 1.09	
15	63.07 ± 0.73	48.45 ± 0.54		24.67 ± 1.11	
18	65.72 ± 0.87	52.58 ± 0.55		29.00 ± 1.34	
21	68.08 ± 1.03	56.17 ± 0.42		33.28 ± 1.66	
24	69.97 ± 0.99	59.03 ± 0.43		38.03 ± 1.81	
38	72.64 ± 1.10	62.95 ± 0.33		43.06 ± 1.81	
48	74.54 ± 1.08	66.68 ± 0.22		46.37 ± 1.91	
72	77.58 ± 1.17	70.74 ± 0.31		50.36 ± 1.06	

3.4 Cell Culture Studies

3.4.1 Development of Drug Resistant Cell Line

Doxorubicin resistant (HeLa/Dox) cell line was developed from parental (HeLa) cell line in our laboratory by gradually increasing drug concentration of medium in which cells grow and proliferate. Starting from the low drug concentration, drug concentration in medium was increased after cells were not affected by certain drug dosage. Finally, HeLa cells became resistant to 500 nM doxorubicin. For the confirmation of resistance, the half maximal inhibitory concentration (IC_{50}) values of doxorubicin, which were determined by XTT cell proliferation assay, for HeLa and HeLa/Dox were compared. IC_{50} value of doxorubicin for parental HeLa cells was 2.725 ± 0.147 μM (Figure 3.13) while IC_{50} value of doxorubicin for HeLa/Dox cells is 100.0 ± 4.5 μM (Figure 3.14).

These results showed that HeLa/Dox cells were 37 times resistant to doxorubicin compared to HeLa cells.

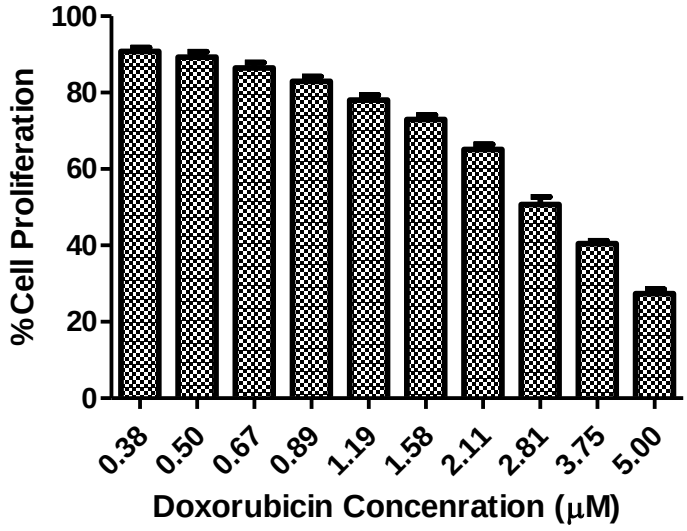

Figure 3.13: Cell proliferation profile of HeLa cells treated with increase in Doxorubicin concentration

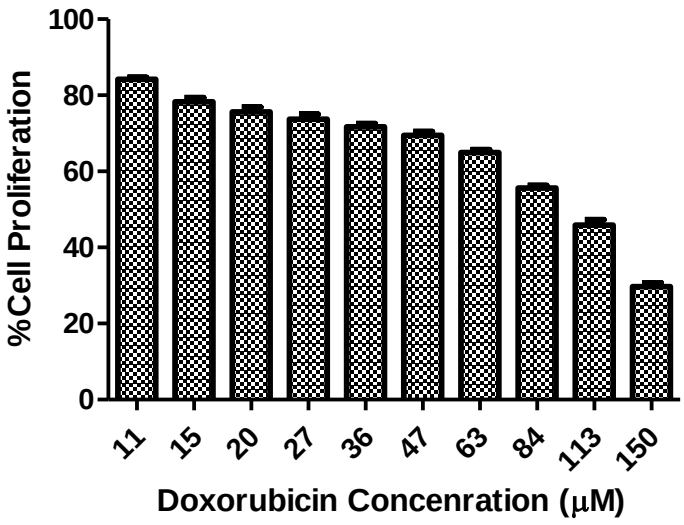

Figure 3.14: Cell proliferation profile of HeLa/Dox cells treated with increase in Doxorubicin concentration

3.4.1.1 Internalization of Nanoparticles

FA-MNPs internalized by HeLa cells were investigated by Purssian blue staining and Dox-FA-MNPs up taken by HeLa were detected by using fluorescent property of doxorubicin under fluorescent microscope.

3.4.1.2 Detection of FA-MNPs in HeLa Cells by Purssian Blue Staining

Purssian blue staining method stains cellular components and iron core of particles in different colors. By this technique, cell and cell components are stained purple while nanoparticles are blue or dark blue in order to observe internalization of the nanoparticles. Different concentrations of FA-MNPs were given to HeLa cells and

incubated at 37^{o}C for 7h. Then, the cells were stained by purssian blue staining method. Increasing concentration of the nanoparticles increased the amount of the particles in the cells (Figure 3.15). Non-treated HeLa cells were seen in only pink color while FA-MNPs-treated HeLa cells were colored as both pink and blue. This result showed that FA-MNPs were internalized by the cells. Also, internalized nanoparticles in low dose were localized together in cells while in highest dosage; they covered all around the cytoplasm. The internalization of nanoparticles by the cells is started as an interaction (adsorbing) followed by vesicle formation and then the formed nanoparticle-containing vesicles are internalized by endocytosis (Osaka. Nakanishi. Shanmugam. Takahama. & Zhang. 2009). The nanoparticles generally were located near nucleus. As a result, it was seen that the particles were endosomally internalized by HeLa cells.

a) b)

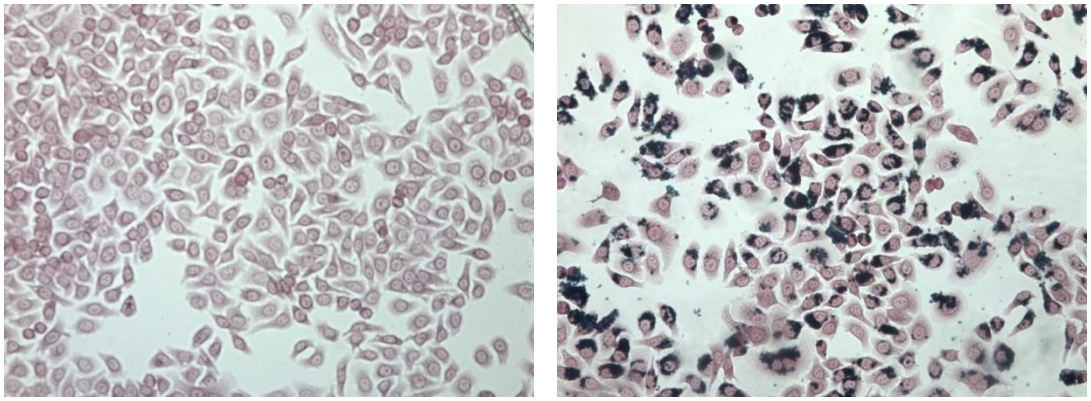

Figure 3.15: Images of HeLa cells treated with 0 µM (a), 25 µg (b), 50 µg (c), 100 µg (d), 150 µg (e) and 200 µg FA-MNPs (f).

c) d)

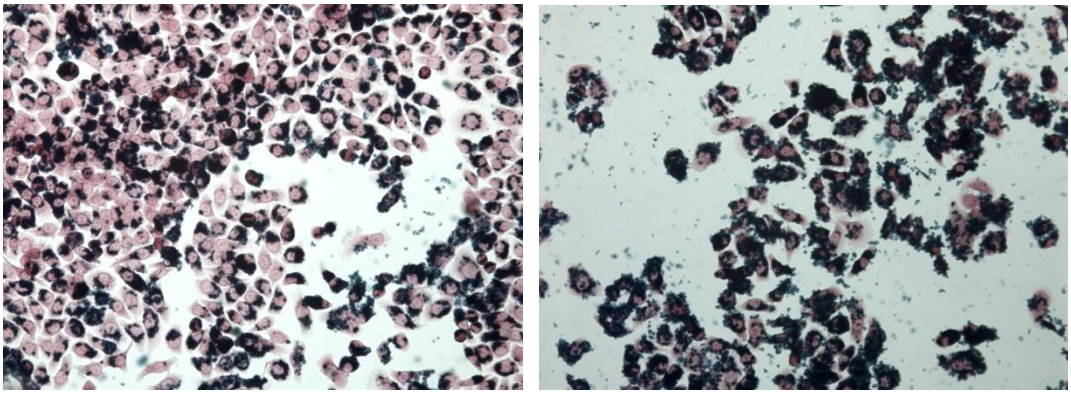

e) f)

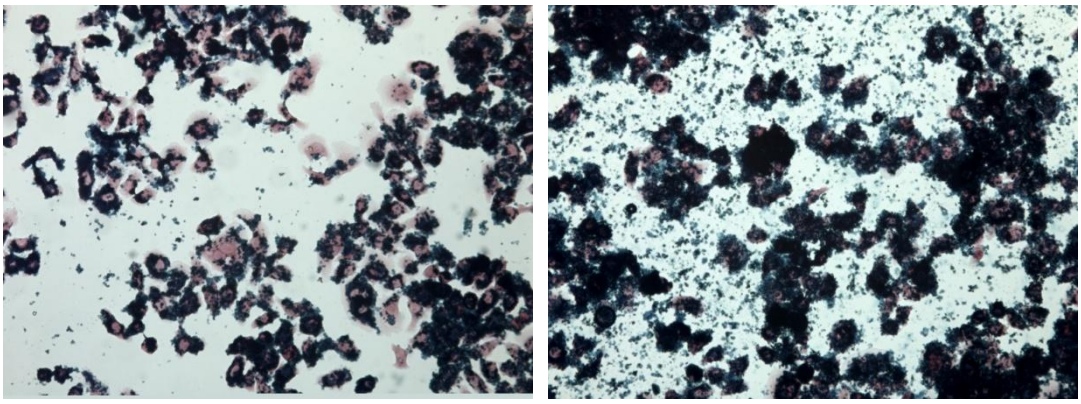

Figure 3.16: Images of HeLa cells treated with 0 µM (a), 25 µg (b), 50 µg (c), 100 µg (d), 150 µg (e) and 200 µg FA-MNPs (f) (Continued).

3.4.1.3 Detection of Dox-FA-MNPs in HeLa Cells by Fluorescent Microscopy

Other detection method for internalized nanoparticles was using the fluorescent property of doxorubicin. As doxorubicin was loaded to FA-MNPs. they gained its fluorescent property. HeLa cells were treated with doxorubicin and different concentration of Dox-FA-MNPs and incubated at 37^{o}C for 7 h. In order to prevent the background fluorescence from non-internalized Dox-FA-MNPs. HeLa cells were extensively washed with PBS. Only doxorubicin treated HeLa cells had fluorescence in their nucleus because doxorubicin targets nucleus while due to endosomal internalization of the particles, there was intense fluorescent emission in cytoplasm of Dox-MNP treated HeLa cells (Figure 3.16).

a) b)

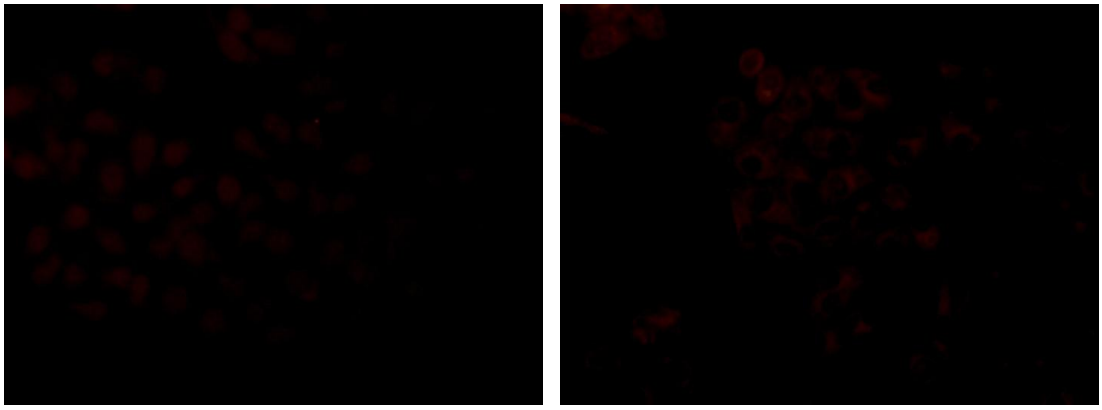

c) d)

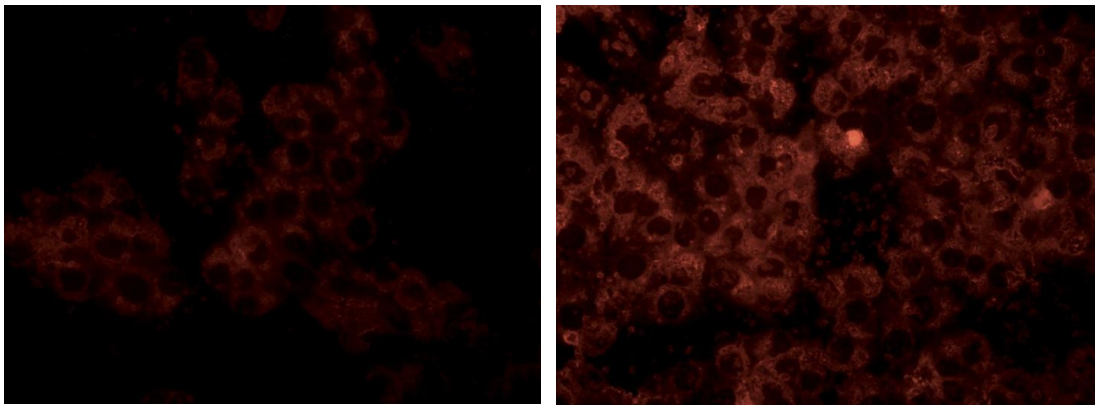

Figure 3.17: Images of HeLa cells treated with doxorubicin (a), 50 µg/mL (b), 150 µg/mL (c) and 200 µg/mL (d) Dox-FA-MNPs.

3.4.2 Antiproliferative Activity of Nanoparticles

The antiproliferative effects of drug loaded MNPs (Dox-MNP) and non-drug loaded MNPs (FA-MNPs) were determined by XTT cell proliferation assay. For this, HeLa and HeLa/Dox cells were treated with different doses (38-500 μg/mL) of FA-MNPs and Dox-FA-MNPs and incubated for 72 h.

The result demonstrated FA-MNPs did not have cytotoxity on HeLa cells while those of Dox-FA-MNPs caused significant decreases on cell proliferation of HeLa cells (Figure 3.17). As a result, FA-MNPs were biocompatible nanoparticles and could be used as drug carriers due to antiproliferative effects of their drug loaded forms.

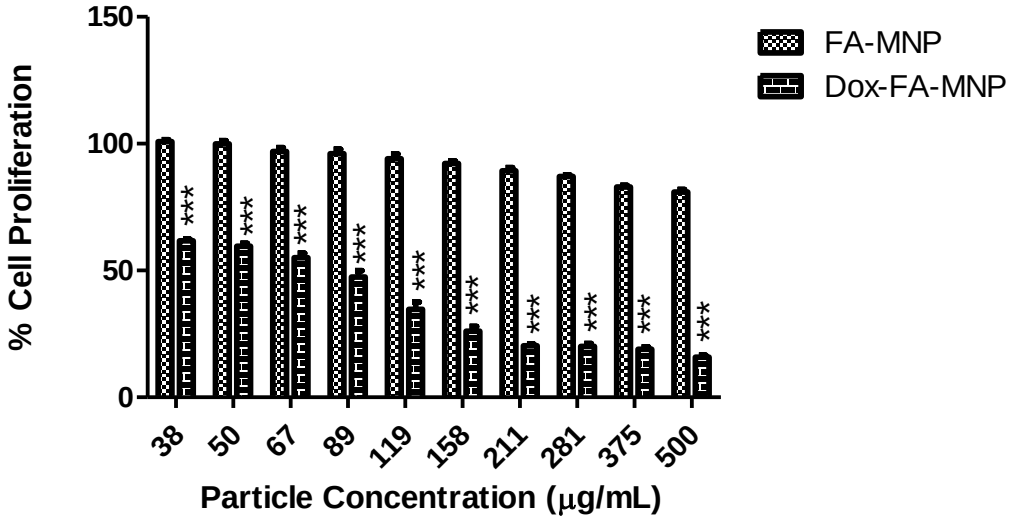

Figure 3.18: Antiproliferative effects of FA-MNPs and Dox-FA-MNPs on HeLa cell line. Results were obtained from three independent experiments, represented as mean ± SEM (* Results were significant with a $p<0.05$).**

Antiproliferative effect of Dox-FA-MNPs on HeLa/Dox cells was investigated by XTT cell proliferation assay in order to see whether particles overcome the drug resistance of the HeLa/Dox cells. XTT dependent cell proliferation assay result showed that Dox-FA-MNPs did not have a significant cytotoxicity on HeLa/Dox cells (Figure 3.18). This could be due to overexpression of P-glycoprotein (cell surface efflux transporter) by doxorubicin in HeLa because doxorubicin upregulates P-gylcoprotein in doxorubicin resistant MCF-7 cells which is main mechanism of multi drug resistance (Dönmez & Gündüz, 2011). Drug release from internalized Dox-FA-MNPs could be slow, so the inner drug concentration could not reach a critical level to kill cells and already released drug in cells could also be pumped outside by transpoter proteins. Therefore, Dox-FA-MNPs could not show cytotoxic effects on HeLa/Dox cells.

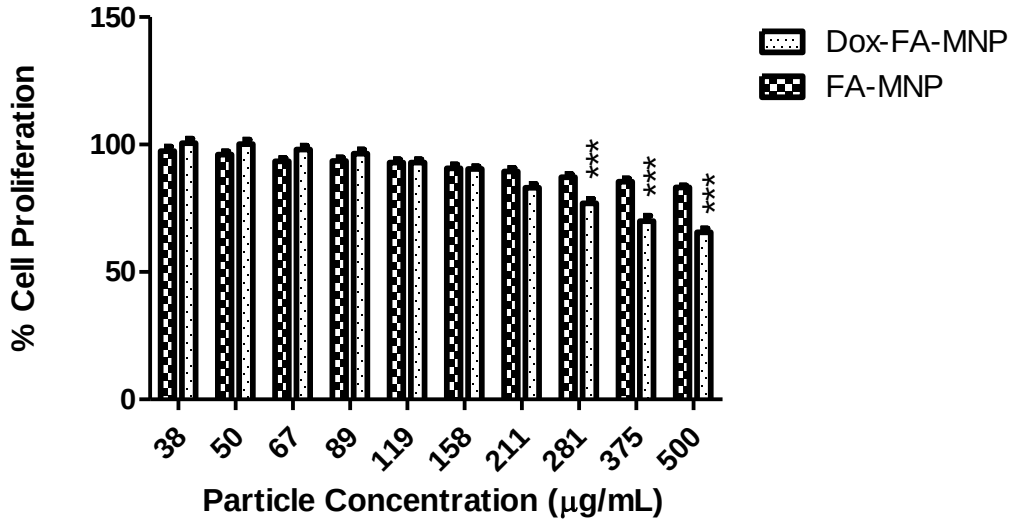

Figure 3.19: Antiproliferative effects of FA-MNPs and Dox-FA-MNPs on HeLa/Dox cell line. Results were obtained from three independent experiments, represented as mean ± SEM (* Results were significant with a $p<0.05$).**

CHAPTER 4

CONCLUSION

1. Synthesized MNPs had approximately 10 nm size and a spherical shape. The core of MNPs contained magnetite (Fe_3O_4). MNPs were also superparamagnetic iron oxide nanoparticles. They had oleic acid and oleylamine on their surface, which made them hydrophobic.

2. MNPs were coated with PEG via hydrophobic interaction between hydrophobic surface of MNPs and hydrophobic part (oleate) of PEG monooleate. FTIR showed MNPs coated with PEG. Size of PEG-MNPs was smaller than 20 nm. Due to PEG coating. PEG-MNPs were bigger than MNPs.

3. FTIR analysis of FA-MNPs indicated the presence of FA conjugated to PEG-MNPs.

4. 505 μM doxorubicin loaded to FA-MNPs was determined after 24 h mixing of FA-MNPs and doxorubicin. 82.27. 75.66 and 114.20 μM doxorubicin released from Dox-FA-MNPs was detected by measurement of absorbance of supernatant at 480 nm after 96 h. Acidity of environment increased the drug release rate when compared the drug releases in two different pH values of acetate buffer. Components of buffer could affects the release of drug compared the drug releases in acetate buffer and dH_2O.

5. Doxorubicin resistant HeLa (HeLa/Dox) cells were developed from parental HeLa cells. HeLa/Dox was 37 times resistant to doxorubicin when compared to HeLa cells according to their IC_{50} values.

6. FA-MNPs and Dox-FA-MNPs were internalized by HeLa cells and Internalization of them was detected by purssian blue staining and by fluorescence of doxorubicin.

7. FA-MNPs were not cytotoxic to HeLa and HeLa/Dox cells. Dox-FA-MNPs effectively showed antiproliferative activity on HeLa cells while they did not show same effect on HeLa/Dox cells.

Doxorubicin loaded folic acid conjugated PEG coated magnetic nanoparticles is effective to kill sensitive cancer cells and may result in decrease in the side effects of doxorubicin.

REFERENCES

American Cancer Society. (2013a). *Different types of chemotherapy drugs*. Retrieved from http://www.cancer.org/treatment/treatmentsandsideeffects/treatmenttypes/chemotherapy/chemotherapyprinciplesanin-depthdiscussionofthetechniquesanditsroleintreatment/chemotherapy-principles-types-of-chemo-drugs Last accessed date: 2014, January 9.

American Cancer Society. (2013b). *What Is Cancer*. Retrieved from http://www.cancer.org/cancer/cancerbasics/what-is-cancer Last accessed date: 2014, January 8.

Arruebo, M., Fernández-pacheco, R., Ibarra, M. R., & Santamaría, J. (2007). Magnetic nanoparticles Controlled release of drugs from nanostructured functional materials ,, *2*(3), 22–32.

Ashley, C. E., Carnes, E. C., Phillips, G. K., Padilla, D., Durfee, P. N., Brown, P. A., … Brinker, C. J. (2011). The targeted delivery of multicomponent cargos to cancer cells by nanoporous particle-supported lipid bilayers. *Nature Materials*, *10*(5), 389–397. doi:10.1038/nmat3042

Attama, A. A., Momoh, M. A., & Builders, P. F. (2012). Lipid Nanoparticulate Drug Delivery Systems : A Revolution in Dosage Form Design and Development.

Berry, C., & Curtis, A. (2003). Functionalisation of magnetic nanoparticles for applications in biomedicine. *Journal of Physics D: Applied Physics*, *198*. Retrieved from http://iopscience.iop.org/0022-3727/36/13/203

Boutry, S., Forge, D., Burtea, C., Mahieu, I., Murariu, O., Laurent, S., … Muller, R. N. (2009). How to quantify iron in an aqueous or biological matrix: a technical note. *Contrast Media & Molecular Imaging*, *4*(6), 299–304. doi:10.1002/cmmi.291

Cancer Council Victoria. (2013). *Cervical Cancer Treatments - Cancer Council Victoria*. Retrieved August 07, 2014, from http://www.cancervic.org.au/about-cancer/cancer_types/cervical_cancer/treatment_for_cervical_cancer.html

Chari, R. V. J. (2008). Targeted cancer therapy: conferring specificity to cytotoxic drugs. *Accounts of Chemical Research*, *41*(1), 98–107. doi:10.1021/ar700108g

Chen, D., Xia, X., Gu, H., Xu, Q., Ge, J., Li, Y., … Lu, J. (2011). pH-responsive polymeric carrier encapsulated magnetic nanoparticles for cancer targeted imaging and delivery. *Journal of Materials Chemistry*, *21*(34), 12682. doi:10.1039/c1jm11195g

Cho, K., Wang, X., Nie, S., Chen, Z. G., & Shin, D. M. (2008). Therapeutic nanoparticles for drug delivery in cancer. *Clinical Cancer Research : An Official Journal of the American Association for Cancer Research*, *14*(5), 1310–6. doi:10.1158/1078-0432.CCR-07-1441

Di Pietro, a, Dayan, G., Conseil, G., Steinfels, E., Krell, T., Trompier, D., … Jault, J. (1999). P-glycoprotein-mediated resistance to chemotherapy in cancer cells: using recombinant cytosolic domains to establish structure-function relationships. *Brazilian Journal of Medical and Biological Research = Revista Brasileira de Pesquisas Médicas E Biológicas / Sociedade Brasileira de Biofísica ... [et Al.]*, *32*(8), 925–39. Retrieved from http://www.ncbi.nlm.nih.gov/pubmed/10454753 Last accessed date: 2014, January 6.

Dönmez, Y., & Gündüz, U. (2011). Reversal of multidrug resistance by small interfering RNA (siRNA) in doxorubicin-resistant MCF-7 breast cancer cells. *Biomedicine & Pharmacotherapy = Biomédecine & Pharmacothérapie*, *65*(2), 85–9. doi:10.1016/j.biopha.2010.12.007

Gkanas, E. I. (2013). In vitro magnetic hyperthermia response of iron oxide MNP's incorporated in DA3, MCF-7 and HeLa cancer cell lines. *Central European Journal of Chemistry*, *11*(7), 1042–1054. doi:10.2478/s11532-013-0246-z

Health News Stories. (2013). Cervical cancer - Treatment - NHS Choices. Retrieved from http://www.nhs.uk/Conditions/Cancer-of-the-cervix/Pages/Treatment.aspx Last accessed date: 2014, August 7.

Ito, A., Shinkai, M., Honda, H., & Kobayashi, T. (2005). Medical application of functionalized magnetic nanoparticles. *Journal of Bioscience and Bioengineering*, *100*(1), 1–11. doi:10.1263/jbb.100.1

Keskin, T. (2012). Preparation of Polyethylene Glycol Coated Magnetic Nanoparticles for Targeting Cancer Cells, (February). Retrieved from http://etd.lib.metu.edu.tr/upload/12614089/index.pdf

Lembo, D., & Cavalli, R. (2010). Nanoparticulate delivery systems for antiviral drugs. *Antiviral Chemistry & Chemotherapy*, *21*(2), 53–70. doi:10.3851/IMP1684

Li, Z., Wei, L., Gao, M. Y., & Lei, H. (2005). One-Pot Reaction to Synthesize Biocompatible Magnetite Nanoparticles. *Advanced Materials*, *17*(8), 1001–1005. doi:10.1002/adma.200401545

Longley, D. B., & Johnston, P. G. (2005). Molecular mechanisms of drug resistance. *The Journal of Pathology*, *205*(2), 275–92. doi:10.1002/path.1706

Lu, A.-H., Salabas, E. L., & Schüth, F. (2007). Magnetic nanoparticles: synthesis, protection, functionalization, and application. *Angewandte Chemie (International Ed. in English)*, *46*(8), 1222–44. doi:10.1002/anie.200602866

Mainardes, R., & Silva, L. (2004). Drug delivery systems: past, present, and future. *Current Drug Targets*. Retrieved from http://www.google.com/patents?hl=en&lr=&vid=USPAT3854480&id=7Z00AAAAEBAJ&oi=fnd&dq=Drug+Delivery+Systems&printsec=abstract

Maity, D., Choo, S.-G., Yi, J., Ding, J., & Xue, J. M. (2009). Synthesis of magnetite nanoparticles via a solvent-free thermal decomposition route. *Journal of Magnetism and Magnetic Materials*, *321*(9), 1256–1259. doi:10.1016/j.jmmm.2008.11.013

Mandal, A. (2014). *What is Chemotherapy*. Retrieved from http://www.news-medical.net/health/What-is-Chemotherapy.aspx Last accessed date: 2014, January 9.

Medical News Today. (2013). *What is folic acid What is vitamin B9 - Medical News Today*. Retrieved from http://www.medicalnewstoday.com/articles/219853.php Last accessed date: 2014, January 8.

Mody, V. V., Cox, A., Shah, S., Singh, A., Bevins, W., & Parihar, H. (2013). Magnetic nanoparticle drug delivery systems for targeting tumor. *Applied Nanoscience*. doi:10.1007/s13204-013-0216-y

National Cancer Institute. (2012). *What You Need To Know About™ Cervical Cancer - National Cancer Institute*. Retrieved from http://www.cancer.gov/cancertopics/wyntk/cervix/page8 Last accessed date: 2014, January 9.

National Cancer Institute. (2013a). *Cervical Cancer Home Page - National Cancer Institute*. Retrieved from http://www.cancer.gov/cancertopics/types/cervical Last accessed date: 2014, January 3.

National Cancer Institute. (2013b). *Cervical Cancer Treatment (PDQ®) - National Cancer Institute*. Retrieved from http://www.cancer.gov/cancertopics/pdq/treatment/cervical/Patient/page4 Last accessed date: 2014, January 9.

National Institutes of Health. (2007). *NIH Curriculum Supplement Series. Biological Sciences Curriculum Study*. Retrieved January 09, 2014, from http://www.ncbi.nlm.nih.gov/books/NBK20362/ Last accessed date: 2014, January 9.

Needham, D., & Dewhirst, M. W. (2001). The development and testing of a new temperature-sensitive drug delivery system for the treatment of solid tumors. *Advanced Drug Delivery Reviews*, *53*(3), 285–305. Retrieved from http://www.ncbi.nlm.nih.gov/pubmed/11744173 Last accessed date: 2014, January 3.

Neuberger, T., Schöpf, B., Hofmann, H., Hofmann, M., & von Rechenberg, B. (2005). Superparamagnetic nanoparticles for biomedical applications: Possibilities and limitations of a new drug delivery system. *Journal of Magnetism and Magnetic Materials*, *293*(1), 483–496. doi:10.1016/j.jmmm.2005.01.064

Osaka, T., Nakanishi, T., Shanmugam, S., Takahama, S., & Zhang, H. (2009). Effect of surface charge of magnetite nanoparticles on their internalization into breast cancer and umbilical vein endothelial cells. *Colloids and Surfaces. B, Biointerfaces*, *71*(2), 325–30. doi:10.1016/j.colsurfb.2009.03.004

Pereyra, A., & Claudia, H. (2013). Gene delivery systems. *Current Issues in Molecular Virology - Viral Genetics and Biotechnological Applicaitons*. doi:10.5772/56869

Schuchter, L. (2014). Side Effects of Chemotherapy [1]. Retrieved from http://www.cancer.net/navigating-cancer-care/how-cancer-

treated/chemotherapy/side-effects-chemotherapy Last accessed date: 2014, August 7.

Sideratou, Z., Kontoyianni, C., Drossopoulou, G. I., & Paleos, C. M. (2010). Synthesis of a folate functionalized PEGylated poly(propylene imine) dendrimer as prospective targeted drug delivery system. *Bioorganic & Medicinal Chemistry Letters*, *20*(22), 6513–7. doi:10.1016/j.bmcl.2010.09.058

Sigma-Aldrich. (n.d.-a). *Folic acid ≥97% Sigma-Aldrich*. Retrieved from http://www.sigmaaldrich.com/catalog/product/sigma/f7876?lang=en&region=TR Last accessed date: 2014, January 9.

Sigma-Aldrich. (n.d.-b). *Poly(ethylene glycol) for molecular biology, average mol wt 8,000 Sigma-Aldrich*. Retrieved from http://www.sigmaaldrich.com/catalog/product/sial/p5413?lang=en&region=TR Last accessed date: 2014, January 9.

Torchilin, V. P. (2001). Structure and design of polymeric surfactant-based drug delivery systems. *Journal of Controlled Release : Official Journal of the Controlled Release Society*, *73*(2-3), 137–72. Retrieved from http://www.ncbi.nlm.nih.gov/pubmed/11516494 Last accessed date: 2014, January 9.

Umut, E. (2013). Surface Modification of Nanoparticles Used in Biomedical Applications. In A. Mahmood (Ed.), *Modern Surface Engineering Treatments*. doi:10.5772/55746

Wedro, B. (2014). *Chemotherapy Treatment Information and Drug Side Effects - MedicineNet*. Retrieved from http://www.medicinenet.com/chemotherapy/article.htm#What_is_chemotherapy Last accessed date: 2014, January 9.

Willis, R. C. (2004). Good things. *Modern Drug Discovery*, (July). Retrieved from http://pubs.acs.org/subscribe/archive/mdd/v07/i07/html/704feature_willis.html Last accessed date: 2014, January 3.

Won, C., Chu, C., & Lee, J. D. O. O. (1998). Synthesis and Characterization of Biodegradable Poly (L -aspartic acid-co-PEG), 2949–2959.

Wu, H., Chang, D., & Huang, C. (2006). Targeted-therapy for cancer. *Journal of Cancer Molecules*, 57–66. Retrieved from http://www.mupnet.com/JOCM 2(2) 57-66.htm

Yallapu, M., Foy, S., Jain, T., & Labhasetwar, V. (2010). PEG-functionalized magnetic nanoparticles for drug delivery and magnetic resonance imaging applications. *Pharmaceutical Research*. Retrieved from http://link.springer.com/article/10.1007/s11095-010-0260-1 Last accessed date: 2014, January 9.

Yang, K., Peng, H., Wen, Y., & Li, N. (2010). Re-examination of characteristic FTIR spectrum of secondary layer in bilayer oleic acid-coated Fe3O4 nanoparticles. *Applied Surface Science*, *256*(10), 3093–3097. doi:10.1016/j.apsusc.2009.11.079

Zhang, J., Rana, S., Srivastava, R. S., & Misra, R. D. K. (2008). On the chemical synthesis and drug delivery response of folate receptor-activated, polyethylene glycol-functionalized magnetite nanoparticles. *Acta Biomaterialia*, *4*(1), 40–8. doi:10.1016/j.actbio.2007.06.006

Zhao, F., Zhang, B., & Feng, L. (2012). Preparation and magnetic properties of magnetite nanoparticles. *Materials Letters*, *68*(01), 112–114. doi:10.1016/j.matlet.2011.09.116

Zwicke, G. L., Mansoori, G. A., & Jeffery, C. J. (2012). targeting of cancer nanotherapeutics, *1*, 1–11.

APPENDIX A

BUFFERS AND SOLUTIONS

A.1. Freezing medium

9ml FBS (Biochrome, Germany)

1ml DMSO (Applichem, Germany)

Mixed and stored at +4°C

A.2. Phosphate buffered saline (pH 7.2)

1 PBS tablet (Sigma. Germany) in 200ml distilled water.

After the tablet dissolved PBS is autoclaved at 121°C for 20 minutes.

A.3. 4X Tris buffer (pH 7)

30.35 g Tris base (Bioshop)

pH is adjusted to 7. Then, volume is completed to 500 mL with distilled water.

A.4. Acetate buffer (pH 4.13. 100 mL)

0.4843 g acetic acid (Sigma)
0.2633 g sodium acetate trihydrate (Sigma)
100 ml water.

A.5. Acetate buffer (pH 5.14. 100 mL)

0.1738 g acetic acid (Sigma)
0.9669 g sodium acetate (Sigma)
100 ml water.

A.6. Acetate buffer (pH 7.4. 100 mL)

0.0013 g acetic acid (Sigma)
1.3578 g sodium acetate (Sigma)
100 ml water.

APPENDIX B

ATR AND FTIR SPECTRA

B.1. Attenuated Total Reflection (ATR) Spectrum of PEGmonooleate

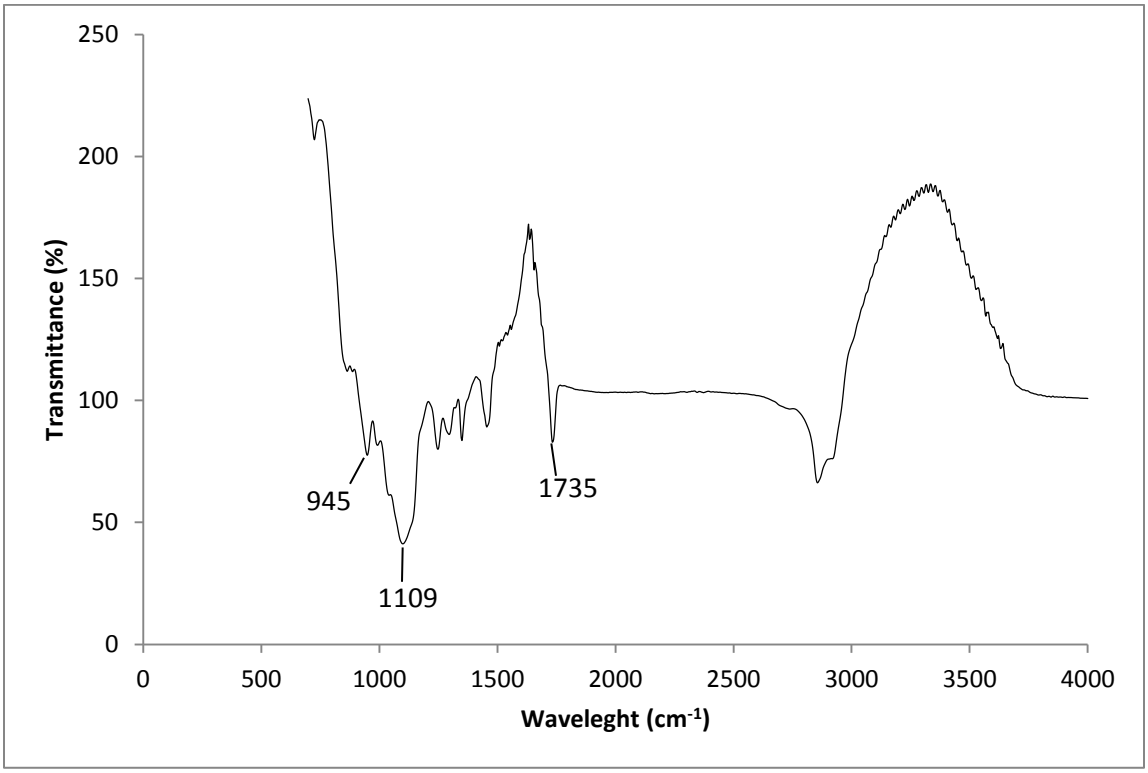

Figure B. 1: ATR Spectrum of PEGmonooleate

The FTIR analyses of PEGmonooleate showed 3 characteristic peaks. The peaks at 946 cm^{-1} and 1109 cm^{-1} indicated the stretching vibration of functional CH_2 group and the stretching vibration of functional group of C–O of PEG respectively while the absorption band observed at 1735 cm^{-1} was caused by C=O carbonyl group of PEG.

B.2. Fourier Transform Infrared Spectroscopy (FTIR) Spectrum of Folic Acid

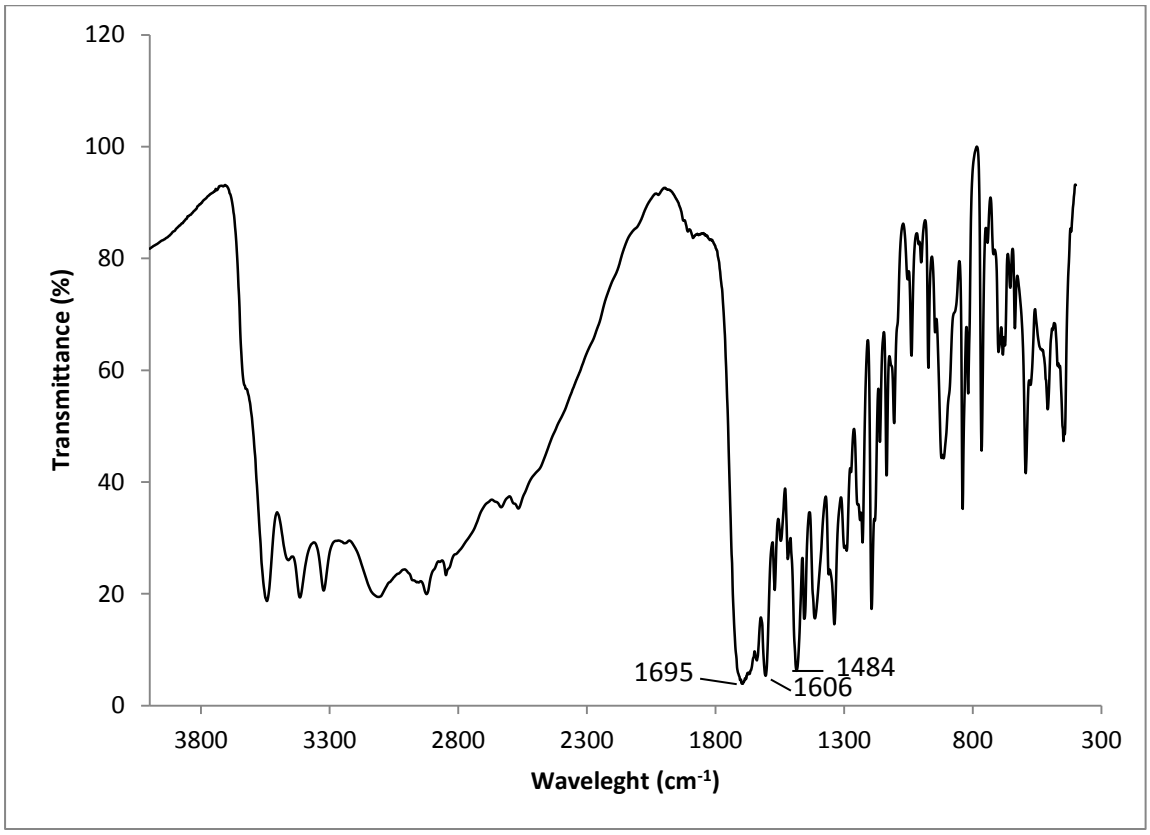

Figure B. 2: FTIR Spectrum of Folic Acid.

The FTIR result showed the characteristic absorption peaks 1433, 1606 and 1695 cm^{-1} of FA. The characteristic band of 1484 and 1411 cm^{-1} were belonging to the phenyl ring of folic acid. 1606 cm-1 band indicated $–NH_2$ bending vibration of FA (Keskin, 2012).

APPENDIX C

CYTOTOXITY OF FA-MNPs ON HeLa AND HeLa/Dox CELL LINES

C.1. HeLa Cell Line

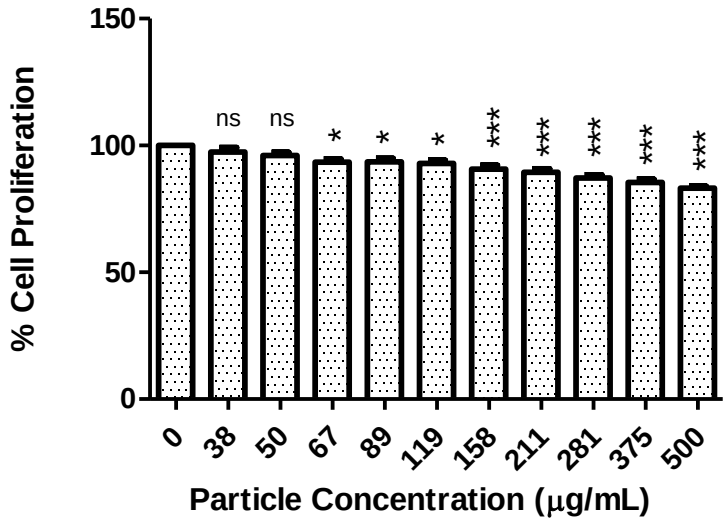

Figure C. 1: Antiproliferative effects of FA-MNPs on HeLa cell line. Results were obtained from three independent experiments. represented as mean ± SEM.

C.2. HeLa/Dox Cell line

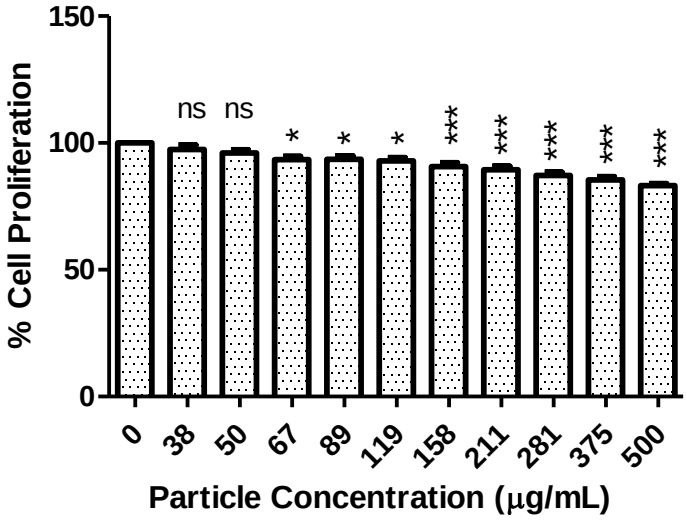

Figure C. 2: Antiproliferative effects of FA-MNPs on HeLa/Dox cell line. Results were obtained from three independent experiments. represented as mean ± SEM.

APPENDIX D

STANDARD CURVE OF DOXORUBICIN

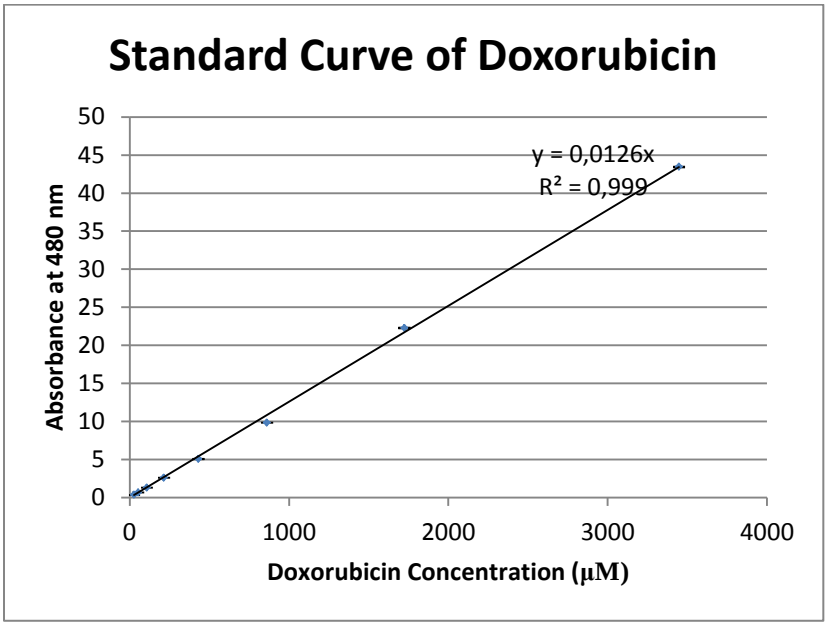

Figure D. 1: Representative standard curve of Doxorubicin.

APPENDIX E

CONCENTRATION OF DOXORUBICIN LOADED TO FA-MNPs

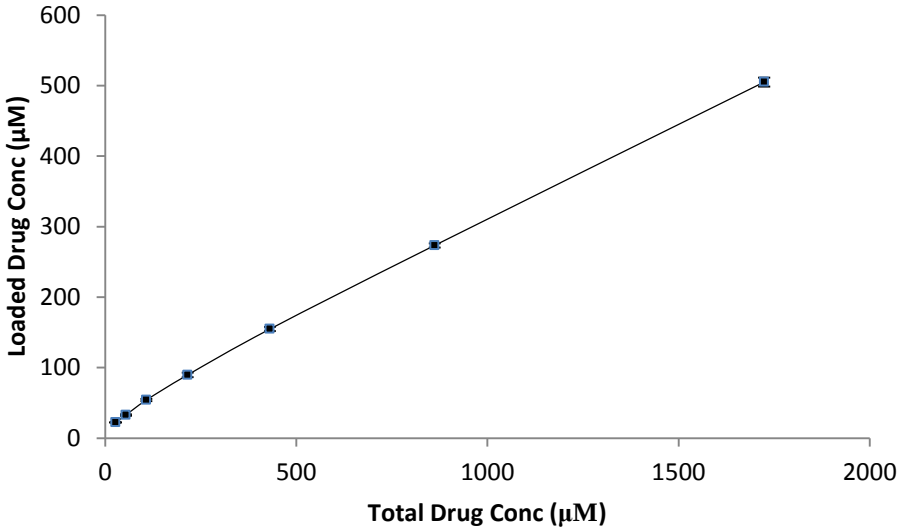

Figure E. 1: Concentrations of Doxorubicin that was loaded to FA-MNPs in different concentrations of Doxorubicin.